

An Inhibitor of the Human UDP-GlcNAc 4-Epimerase Identified from a Uridine-Based Library: A Strategy to Inhibit O-Linked Glycosylation

Katharine A. Winans^{1,5} and Carolyn R. Bertozzi^{1,2,3,4}

¹Center for New Directions in Organic Synthesis
Department of Chemistry
University of California, Berkeley, California 94720

²Department of Molecular and Cell Biology

³Howard Hughes Medical Institute
University of California, Berkeley
Berkeley, California 94720

Summary

The biological study of *O*-linked glycosylation is particularly problematic, as chemical tools to control this modification are lacking. An inhibitor of the UDP-GlcNAc 4-epimerase that synthesizes UDP-GalNAc, the donor initiating *O*-linked glycosylation, would be a powerful reagent for reversibly inhibiting *O*-linked glycosylation. We synthesized a 1338 member library of uridine analogs directed to the epimerase by virtue of substrate mimicry. Screening of the library identified an inhibitor with a K_i value of 11 μ M. Tests against related enzymes confirmed the compound's specificity for the UDP-GlcNAc 4-epimerase. Inhibitors of a key step of *O*-linked glycan biosynthesis can be discovered from a directed library screen. Progeny thereof may be powerful tools for controlling *O*-linked glycosylation in cells.

Introduction

The carbohydrate chains that adorn membrane proteins have emerged as key players in the information transfer that takes place at the cell surface. Leukocyte recruitment to sites of inflammation, cell adhesion to the extracellular matrix during development, and the sperm-egg recognition that initiates fertilization all demand the appropriate carbohydrate participant [1–3]. Furthermore, aberrant glycan structures mediate disease states such as chronic inflammation and cancer metastasis [4]. Despite compelling examples of the physiological roles that protein-bound saccharides may play, in general, structure-function correlations for glycans have lagged dramatically behind an analogous understanding of the protein proper. While the techniques of molecular biology—site directed mutagenesis, gene knockouts, and the like—have revolutionized our comprehension of protein science, oligosaccharide assembly defies the analogous manipulation. Carbohydrate chains are assembled on either asparagine (*N*-linked glycosylation) or serine or threonine residues of proteins (*O*-linked glycosylation) in sequences that vary with the efficiency of the glycosylating enzymes; the glycoprotein product thus is not a discrete structure, but rather an array of glycoforms. The heterogeneity that characterizes glycans complicates

structure-function analysis and compromises our ability to decipher the important physiological functions these structures may perform.

Study of *O*-linked glycosylation has suffered particularly in this regard. The basic ability to inhibit the process at will—so crucial to experiments testing the significance of *O*-linked glycans in a particular physiological transaction—so far eludes us. While, for the *N*-linked modification, abolition of glycosylation by site-directed mutagenesis of consensus sites in the acceptor protein represents a routine strategy [5–7], no analogous consensus sequence directing *O*-linked initiation exists. The family of transferases catalyzing the initial transfer of an *N*-acetylgalactosamine (GalNAc) residue from the high-energy donor, UDP-GalNAc, to a serine or threonine on the acceptor protein possesses poorly defined and overlapping preferences for the acceptor protein's sequence [8, 9]. Serines and threonines typically abound near *O*-linked sites; their prevalence impedes identification of a glycan's precise amino acid host and implies that loss of a known *O*-linked locale may simply divert the carbohydrate to a nearby, normally vacant site [10].

Chemical control of *O*-linked glycosylation in cultured cells is also limited; a solitary reagent, α -benzyl GalNAc, comprises the entire arsenal. This compound serves as an alternative substrate for enzymes that modify the initial, monoglycosylated protein, curtailing elaboration of *O*-linked glycans beyond the monosaccharide GalNAc [11]. Unfortunately, broad use of α -benzyl GalNAc has been limited because the compound represents a potentially toxic cell culture additive at the millimolar concentrations required, and allows the protein to retain its important, proximal GalNAc residue. In contrast, the study of *N*-linked glycans profits from the glycosylation inhibitor tunicamycin, a compound originally identified for its antiviral properties that blocks the synthesis of the carbohydrate donor for *N*-linked glycosylation with nanomolar efficiency [12]. In addition, a potent inhibitor of the solitary oligosaccharyl transferase that initiates *N*-linked glycosylation offers the promise of highly selective interruption of this posttranslational modification [13]. The benefit to *N*-linked glycan research of such tools has been marked, suggesting to us that an analogous chemical tool for *O*-linked research would prove valuable.

As a broad scheme to enhance our ability to analyze the functional significance of *O*-linked protein glycosylation, we therefore sought to develop an inhibitor of this process. A natural focus might have been the enzyme(s) responsible for installing the initial monosaccharide, GalNAc, onto the fledgling glycoprotein. However, the cohort of GalNAc transferases performing this task—8 mammalian genes characterized so far—comprised a complicated target [8, 14]. Thus, we looked upstream to the biosynthesis of UDP-GalNAc, the carbohydrate donor itself. Our attention centered on the UDP-GlcNAc 4-epimerase (called 4-epimerase hereafter), which catalyzes the conversion of the common nucleotide sugar UDP-GlcNAc to the *O*-linked precursor, UDP-GalNAc;

⁴ Correspondence: bertozzi@cchem.berkeley.edu

⁵ Present address: Department of Medicine, Division of Infectious Diseases and Geographic Medicine, Stanford University Medical Center, Stanford, California 94305.

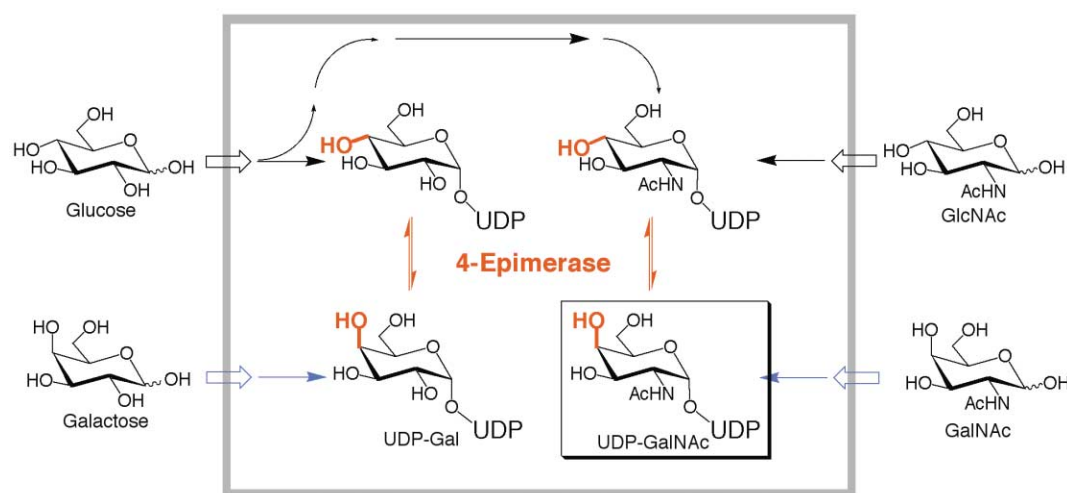


Figure 1. Biosynthesis of UDP-GalNAc, the Initial Carbohydrate Donor in O-Linked Glycosylation

The major route to cellular UDP-GalNAc is via exogenous Glc and GlcNAc, both of which can be converted to UDP-GlcNAc. Epimerization at the C-4 position (in red) by our target enzyme, the UDP-GlcNAc 4-epimerase, yields UDP-GalNAc. The same epimerase converts UDP-Glc to UDP-Gal. Salvage pathways (blue arrows) enable the cell to take up Gal and GalNAc and convert them directly to their UDP-linked derivatives.

inhibiting this conversion would be expected to curtail O-linked glycosylation altogether (Figure 1). We reasoned that since GalNAc expression on proteins is largely limited to O-linked glycans—its reported incorporation into N-linked structures is rare, confined to the terminal elaborations of certain pituitary glycopeptide hormones [15–17]—the effects of our potential UDP-GalNAc inhibitor would be appropriately selective. Indeed, experiments by Krieger and coworkers with a Chinese hamster ovary (CHO) cell line deficient in 4-epimerase activity, the “IdID” cell line, demonstrate that O-linked glycans may be inhibited to the exclusion of their N-linked counterparts [18, 19].

One complication to this simple paradigm should be noted. Mammalian forms of the 4-epimerase also convert UDP-Glc to UDP-Gal (Figure 1) [20]. While GalNAc expression is largely limited to O-linked glycans, Gal participates more widely; it comprises, for example, part of the LacNAc (Gal β 1-4GlcNAc) disaccharide commonly appended as long chains in complex-type N-linked glycans [21]. 4-Epimerase inhibition would then affect both N- and O-linked structures. Fortunately, nature provides a safety valve; salvage pathways enable the cell to utilize the free monosaccharides Gal and GalNAc to generate their UDP-linked derivatives (Figure 1). By supplying exogenous Gal to cultured cells treated with inhibitor, we should selectively impede O-linked glycosylation while leaving N-linked structures intact (Figure 2). Treatment with inhibitor without either Gal or GalNAc should truncate complex and hybrid type N-linked structures, and abolish O-linked glycans altogether. Finally, application of Gal and GalNAc to inhibitor-treated cells should rescue both types of glycosylation. Experiments using the 4-epimerase-deficient IdID cells yield just this pattern of data, supporting our choice of target enzyme [18, 19]. Furthermore, the viability of these cells when exogenous sugars are limiting supports our hypothesis that 4-epimerase inhibition would be tolerated. We predict that

blockage of the 4-epimerase will provide a flexible tool for modulating protein glycosylation in any cultured cell line of interest.

Having identified our target enzyme, our immediate task became the efficient design of an inhibitor. To date, the most potent inhibitors of enzymes operating on UDP-linked carbohydrates have been rationally designed substrate or transition-state analogs [22–26]. These compounds incorporate the UDP component of

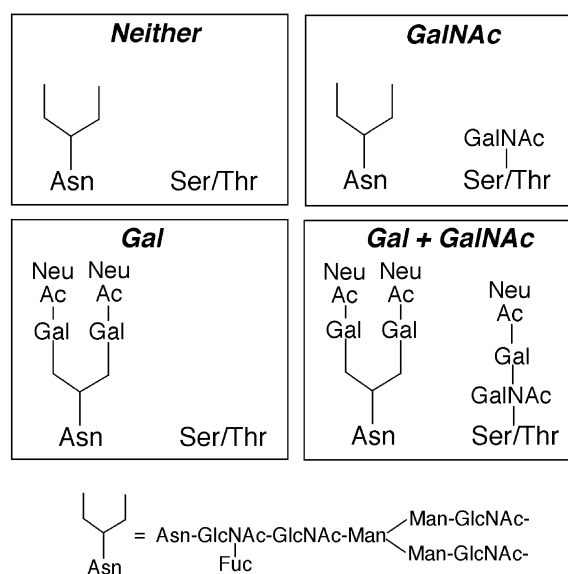


Figure 2. Expected N- and O-Glycan Structures in the Presence of a UDP-GlcNAc 4-Epimerase Inhibitor

For each panel, the designation in bold indicates the presence or absence of exogenous Gal or GalNAc. When only exogenous Gal is added (lower left panel), selective inhibition of O-linked glycosylation should be observed, with N-linked glycans unaffected. Adapted from [18].

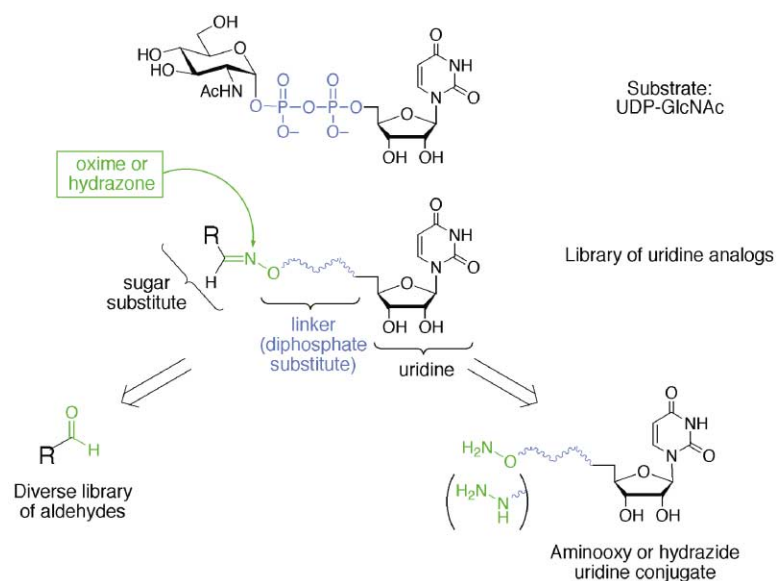


Figure 3. General Strategy for Uridine Library Synthesis

Aminoxy- and hydrazone-functionalized uridine forms the common library scaffold; variety is installed by reaction of the uridine derivative with a library of aldehydes chosen for their diversity and favorable pharmacological properties. The selective nature of oxime or hydrazone formation (indicated in green) allows the incorporation of a wide array of functionality on library aldehydes without the need for protecting groups and their attendant complications. Three different linkers (indicated in blue) were designed as potential diphosphate substitutes.

the native substrate, while altering the sugar structure to abolish turnover or enhance binding. While such strategies have generated inhibitors with potencies in the micromolar range—affinities that rival those of the substrates—the winning compounds are unsuitable for use *in vivo*, since their highly polar or even charged structures would be membrane impermeable. We thus sought to develop an expedient method to capitalize on the inherent binding affinity of the 4-epimerase for its substrate, while simultaneously optimizing the pharmacological properties of the potential inhibitor.

Our strategy exploited a key chemoselective coupling between a uridine derivative functionalized at its 5' position by an aminoxy or hydrazone group and a diverse array of commercially available aldehydes, which yielded the corresponding oxime- or hydrazone-based libraries (Figure 3). The highly selective natures of oxime and hydrazone bond formation make them suited for biological applications in which specific reactions are desired

amidst a complex, richly functionalized backdrop. The technique has been employed in peptide synthesis [27, 28], cell surface engineering [29, 30], and, more recently, chemical library synthesis [31]. Taking our cue from these pioneering works, we employed chemoselective ligation as a facile mechanism to diversify the uridine-based library, and thereby optimize the substituent occupying the carbohydrate binding pocket of the 4-epimerase. The uridine derivatives were readily generated on multigram scale, which allowed for tuning of the linker region to facilitate binding by aldehyde-derived substituents.

We report herein the initial phase of this project: the synthesis and screening of uridine-derived libraries against the human 4-epimerase. From these libraries a hit compound designated **1-143** was identified, with a K_i versus the substrate UDP-Gal of 11 μ M. *In vitro* tests of this compound's potency against a panel of related enzymes demonstrate the specificity of the hit compound

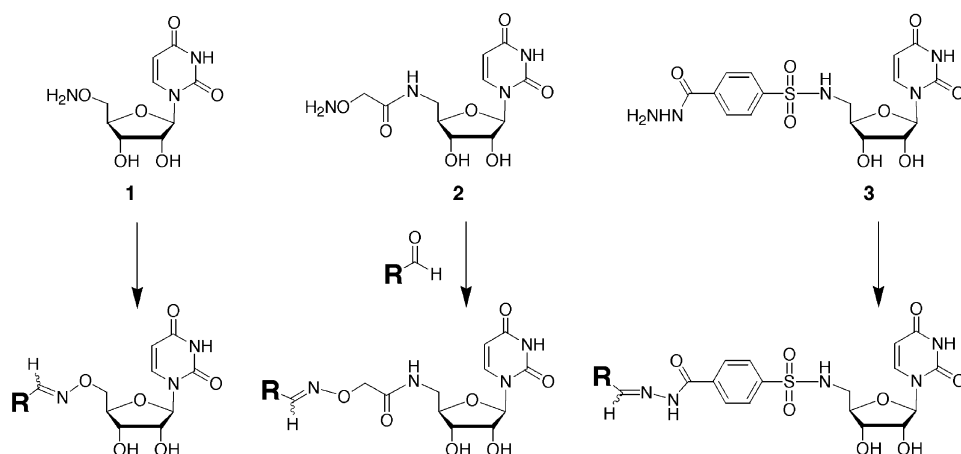


Figure 4. Aminoxy- and Hydrazone-Functionalized Uridine Derivatives Used in Library Synthesis

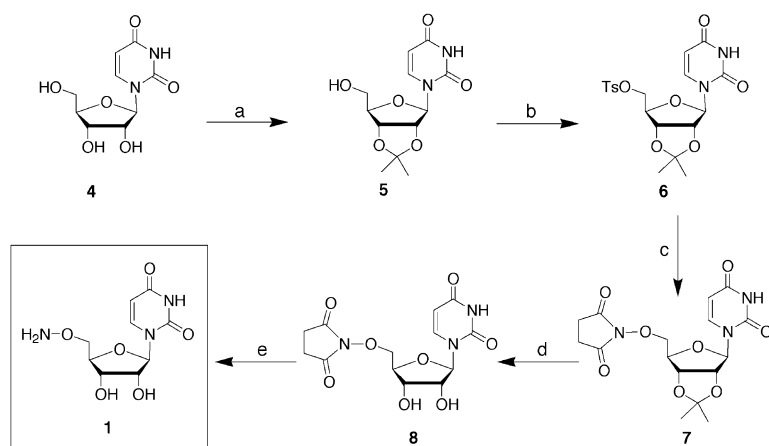


Figure 5. Synthesis of 5'-Aminoxy-Uridine 1
a, 2,2-dimethoxypropane, TsOH, DMF; b,
Ts₂O, pyr, CH₂Cl₂; c, NHS, DIEA, DMF; d, 90%
TFA/H₂O; e, 40% MeNH₂/H₂O:MeOH (2:1).

for its target enzyme, the 4-epimerase, and suggest that testing of this compound as an inhibitor of O-linked glycosylation in cultured cells would be warranted.

Results

Synthesis of Aminoxy- and Hydrazide-Functionalized Uridine Derivatives

Our initial challenge was to design and synthesize appropriate uridine derivatives (Figure 4). We chose three linking structures to unite the uridine component with its aldehyde partner in order to explore the significance of varied length, flexibility, and hydrogen-bonding potential to inhibitor potency. Data of UDP-Gal complexed with the *E. coli* 4-epimerase reveal hydrogen bonding interactions between the substrate's phosphate groups and three amino acid side chains [32]. In our linkers we sought to incorporate analogous hydrogen bond acceptors; we postulated that the amide and sulfonyl moieties of 2 and 3, respectively, would fulfill this goal (Figure 4). Both carbonyl and sulfonyl groups have been used successfully as phosphate substitutes [33, 34]. Indeed, the sulfonyl benzoyl group's aptitude as a diphosphate mimic has been documented in a 54 nM inhibitor of the EGF-receptor protein tyrosine kinase [35]. Because the diversity inherent in our aldehyde collection made predicting a preferred linker length impossible, we installed corresponding diversity in the linker, choosing structures ranging from one (1) to six bonds (3) between the 5' uridine substituent and the oxime or hydrazone nitrogen. We speculated that compound 2 would display slightly enhanced flexibility due to the methylene proximal to its aminoxy group.

To achieve the most efficient syntheses of the three uridine targets, we designed routes using common intermediates where it was practical; thus, compounds 1-3 all derived from the activated 5'-O-toluenesulfonyl uridine derivative 6 (Figure 5). This compound was generated by treatment of uridine (4) with 2,2-dimethoxypropane and TsOH in DMF to afford 2',3'-O-isopropylidene uridine (5) in 89% isolated yield. Tosylation was achieved in routine fashion. To produce the initial uridine target 1, the tosylate was displaced with NHS to yield compound 7. Two deprotection steps followed, producing

1 in 38% yield over the five-step synthesis after HPLC purification.

The latter two targets, compounds 2 and 3, both derived from 5'-aminouridine 11 (Figure 6). Installation of the nitrogen functionality was achieved by reacting the common intermediate, 5'-O-toluenesulfonyl uridine derivative 6, with lithium azide. Ensuing chemistry required the reduction of azidouridine 9 to the amino compound. Interestingly, in our hands 5'-azido-2',3'-O-isopropylidene uridine (9) was entirely resistant to reduction; this experience contrasts with previous reports in which this compound was successfully reduced by hydrogenation [22]. Acid hydrolysis of the isopropylidene yielded the free azido sugar 10, which we found was easily reduced to 5'-aminouridine 11 by Pd-catalyzed hydrogenation. The overall yield for production of 5'-aminouridine 11 from free uridine in five steps was 80%, an efficiency that allowed ample production of subsequent uridine derivatives.

Synthesis of the second target, 5'-aminoxy-glycyl-uridine 2, was completed by an EDC and HOBt-mediated coupling of the intermediate 5'-aminouridine 11 with (*t*-BOC-aminoxy)acetic acid. Deprotection of 12 and purification by HPLC afforded 5'-aminoxy-glycyl-uridine 2 in 41% yield over the final two steps. Our final target, 5'-hydrazido-phenylsulfonyl-uridine 3, was also prepared using the 5'-aminouridine (11) intermediate; in this case a coupling with methyl ester 13 installed the desired linker (Figure 7). The coupled product 14 was saponified using lithium hydroxide, then an EDC and HOBt-mediated coupling to *t*-BOC hydrazide yielded compound 15. Finally, deprotection and HPLC purification yielded uridine target 3 in 37% yield over four steps.

Synthesis and Characterization of Uridine-Derived Libraries

The successful synthesis of uridine derivatives 1-3 and the purchase of 446 commercially available aldehydes provided the building blocks for our library of uridine conjugates (Figure 4). To determine appropriate reaction conditions for library synthesis, we monitored by ¹H NMR a sample of 33 oxime and hydrazone-forming reactions. Figure 8 depicts three examples. Reaction progress was observed by following the disappearance of the alde-

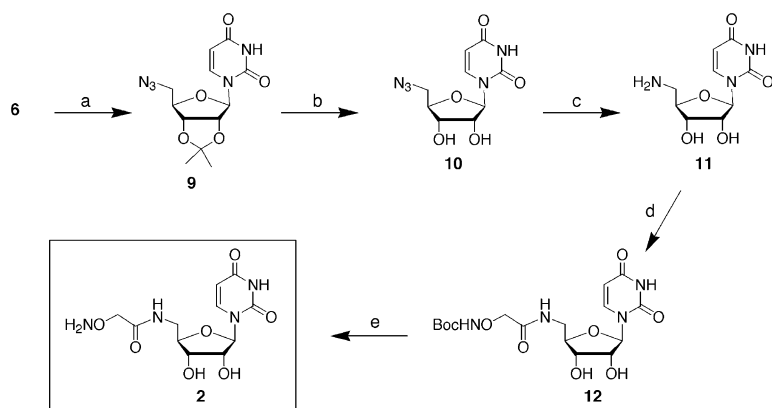


Figure 6. Synthesis of 5'-Aminoxy-Glycyl-Uridine 2

a, LiN_3 , DMF; b, 90% TFA/ H_2O ; c, H_2 , Pd/C, MeOH; d, (t-BOC-aminoxy)acetic acid, EDC, HOBt, DMF; e, 40% TFA/ CH_2Cl_2 .

hyde proton resonance (typically found between 8.5 and 11.0 ppm) and the corresponding appearance of oxime or hydrazone proton resonance (typically between 7.0 and 9.5 ppm). The identities of the coupled products were confirmed by mass spectrometry; stereochemistry about the oxime or hydrazone double bond was not determined. Reactions were performed at room temperature, with substrates at 0.1 M in 1% AcOH in d_6 -DMSO. We found that most were complete within 12 hr, as shown in Figure 8; almost all observed were complete within 2 days. Hydrazone-forming reactions with uridine derivative 3 tended to proceed slightly more slowly than the corresponding oxime formations; three such reactions required 4 days to complete. Of the 33 reactions followed in this manner, all but four afforded yields of 80% or better (Table 1). All products, observed under these conditions for a total of 7 days, were found to be stable for the duration of the experiment. We thus observed that these coupling reactions were highly efficient, confirming their utility for the large-scale library production we planned.

Limited quantities of 300 aldehydes prohibited the type of ^1H NMR experiments described above and necessitated that oxime and hydrazone coupling reactions be executed at 0.01 M rather than 0.1 M as performed previously. To characterize coupling efficiencies under these conditions, we monitored reaction progress by reversed-phase HPLC. We quantitated yields after 72 hr by measuring the percent reduction of a peak corresponding to uridine derivative 1, 2, or 3, while observing

the corresponding appearance of oxime or hydrazone product (Table 1). The identities of the coupled products were confirmed by mass spectrometry. The presence of side products precluded this method of yield determination in several cases, indicated with an asterisk in Table 1. Dilute concentrations of reagents appeared to affect the coupling negligibly; these reactions were highly efficient and clean, producing yields of 80% or better in 85 out of 99 reactions tested. Cases in which yields lagged often correlated with incomplete dissolution of the aldehyde in the reaction mixture.

Screening of Uridine Libraries against UDPGlcNAc 4-Epimerase

With the uridine-derived library in hand, we pursued our larger goal of identifying potential inhibitors of the 4-epimerase. The 1338 library compounds were screened against the 4-epimerase using a coupled-enzyme system with a spectrophotometric readout (Figure 9). The compounds were assayed at 100 μM , in the presence of 100 μM —the K_m concentration—of the 4-epimerase substrate, UDP-Gal. Initial screens identified 39 compounds displaying 30% inhibition or better (Figure 10). We were interested to observe that while we identified a significant number of initial hits, enzyme binding was quite specific; despite the common uridine scaffold, over 1000 library members inhibited the 4-epimerase by less than 10% (data not shown). This suggested to us that any 4-epimerase inhibitor identified might possess specific affinity for this

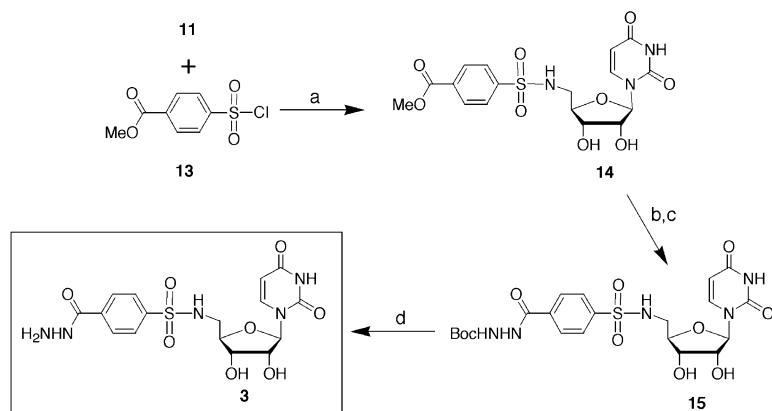


Figure 7. Synthesis of 5'-Hydrazide-Phenyl-sulfonyl-Uridine 3

a, TEA, DMF; b, LiOH, MeOH: H_2O (3:1); c, t-BOC-hydrazide, EDC, HOBt, DMF; d, 40% TFA/ CH_2Cl_2 .

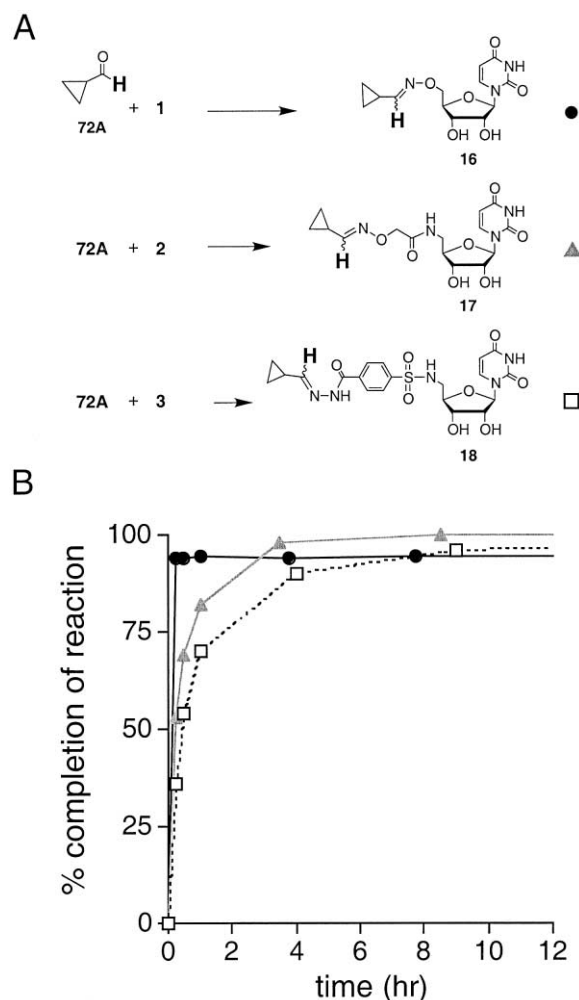


Figure 8. Time Courses of Three Library Coupling Reactions, as Monitored by ^1H NMR

(A) Coupling reactions observed.

(B) Reaction progress as assessed by comparing the relative intensity of the aldehyde proton resonance (72A, H depicted in bold) to that of the product oxime or hydrazone proton resonance (16–18, H depicted in bold).

enzyme rather than simple cross-reactivity with any proteins that bound uridine.

Preliminary inspection of the initial hit structures appeared to favor compounds derived from uridine analog 3 (Figure 10). Of 39 hit compounds, 27 originated with analog 3. This trend withered in follow-up experiments in which we rescreened the compounds (Figure 11) or measured their IC_{50} values. Because our assay employed spectrophotometric detection of enzyme activity, the data could be convoluted by the absorbance or solubility properties of library compounds themselves. We observed, for example, that library members derived from compound 3 were more often strongly light absorbent or insoluble in the assay mixture than their counterparts derived from uridine analogs 1 or 2. In our rescreening protocol, we accounted for such artifacts by preincubating the enzyme mixture with the library compound and achieving a stable baseline absorbance be-

fore initiating the reaction. (To perform the assay in this manner for all 1338 compounds in the initial screen was impractical and unnecessary. The protocol is described in detail in the Experimental Procedures section.)

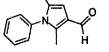
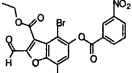
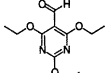
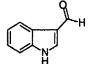
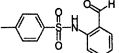
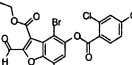
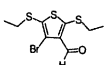
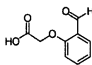
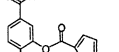
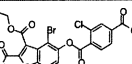
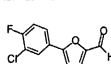
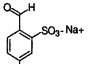
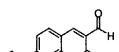
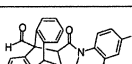
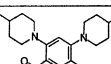
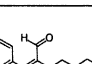
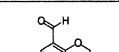
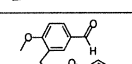
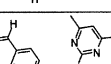
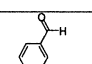
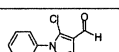
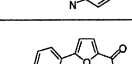
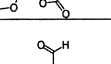
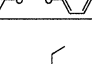
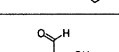
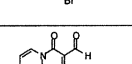
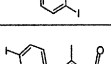
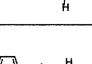
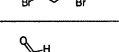
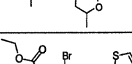
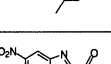
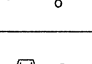
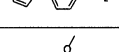
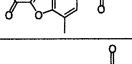
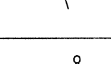
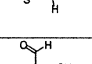
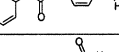
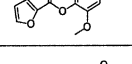
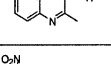
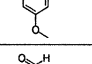
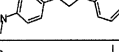
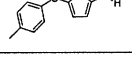
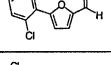
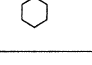
Having weeded our results of false positives, we observed no trend favoring library compounds made from one uridine derivative (1, 2, or 3) over the others. A solitary compound, designated 1-143, prevailed strikingly; while this compound inhibited 4-epimerase activity by 78% upon rescreening, no other hits surpassed 35% inhibition. Thus, despite the library's common uridine scaffold, the 4-epimerase substrate binding pocket exhibited marked selectivity. As depicted in Figure 11, potency of compound 1-143 demanded the appropriate linker between the uridine and aldehyde derivatives; union of aldehyde 143 with uridine derivative 2 or 3 yielded essentially inactive compounds.

Synthesis and Characterization of Hit Compound 1-143

To further assess the inhibitory activity of compound 1-143, we resynthesized it on a larger scale (Figure 12). Theoretically, our product could adopt either the *E* or *Z* configuration about the oxime bond. In our synthesis, we observed two product isomers distinguishable by both HPLC and ^1H NMR; one was favored overwhelmingly, comprising approximately 90%–95% of the total product yield. As energetics should favor the *E* configuration, we predicted that this was our major isomer. Previous researchers synthesizing an oxime library have noticed a similar trend (Dustin Maly, personal communication; [31, 36]). Chemical shifts of the oxime protons for the two isomers supported this assignment; for the major isomer, the oxime singlet appeared downfield of its minor counterpart (8.94 ppm versus 7.90 ppm), which we and others have observed as characteristic positioning for *E* versus *Z* oxime protons [37, 38].

Interestingly, during the course of this synthesis and purification, we observed that the two isomers would interconvert in a light-dependent fashion. While the oxime-forming reaction favored production of the *E* isomer—as mentioned previously, 90%–95% of the product was in this configuration—upon extended exposure to light the relative ratios of the isomers would reverse, coming to an equilibrium of approximately 65:35 after 5 days. This effect was definitively dependent on light; ^1H NMR at temperatures up to 70°C detected no alterations in the isomeric mixture. The interconversion of isomers that we noticed parallels previous reports for both alkenes and oximes; UV light may isomerize the thermodynamically favored *E* form to yield the *Z* isomer [39]. We speculate that the highly conjugated nature of 1-143 allows it to undergo this conversion using visible light. While overall the conversion we observed was slow, occurring on the order of days, when we purified the *E* isomer we found it to be contaminated with a small proportion of the *Z* isomer (for example, 96% *E* with 4% *Z*). Thus, purified material we used in subsequent enzymatic assays did contain both isomers; we hypothesize, but cannot state definitively, that the *E* isomer represents the active form.

Table 1. Yields for Representative Library Couplings

	1	2	3		1	2	3		1	2	3		1	2	3
	98	81	85		*	*	97		97	99	94		86	87	50
	97	96	97		97	98	96		97	70	69		88	99	85
	99	94	95		*	79	97		97	*	96		95	94	83
	99	95	97		97	88	89		97	93	88		94	73	57
	99	87	90		97	95	90		*	*	*		91	99	89
	97	93	95		97	91	94		96	98	97		95	99	91
	97	92	96		97	59	58		96	85	86		78	97	88
	97	67	45		97	*	*		97	99	97		81	80	80
	97	98	96		97	98	97		94	98	97		85	99	91
	18	17	14		95	97	96		97	98	96		90	99	92
	97	*	*		97	95	97		97	93	95		95	99	99

Values in italics are derived from ¹H NMR experiments in which reaction progress was quantitated by comparing the relative intensities of the aldehyde and oxime or hydrazone proton resonances. All other values were measured by RP-HPLC experiments in which reaction progress was followed by the disappearance of a peak corresponding to the uridine starting material and the coincident appearance of a product peak. Asterisks denote reactions in which the presence of side products precluded this method of yield determination.

Inhibitory Activity of Purified 1-143 against the 4-Epimerase

We used the purified 1-143 to define the compound's activity against the 4-epimerase. Because our 4-epimerase assay employs an accessory enzyme—the UDP-Glc dehydrogenase—we were anxious to determine whether inhibition of that enzyme accounted for the activity we had observed. We performed IC₅₀ measurements for both enzymes, in each case using substrate concentrations equal to the K_m value (4-epimerase, UDP-Glc, 100 μM; dehydrogenase, UDP-Glc, 20 μM). As portrayed in Figure 13, compound 1-143 was strikingly specific for the 4-epimerase; the UDP-Glc dehydrogenase retained its full activity even at 200 μM inhibitor, whereas the 4-epimerase activity was reduced to 10% under analogous conditions.

To evaluate whether the two subunits from which 1-143 was derived—uridine analog 1 and aldehyde 143—themselves inhibited the 4-epimerase, we assayed each one separately. Assays were performed using 100 μM UDP-Glc, and up to 2 mM of either 1 or aldehyde 143. Even at these elevated concentrations, neither subunit demonstrated appreciable inhibitory activity; the 4-epimerase retained 100% activity in the presence of 2 mM uridine analog 1 and 72% activity at 2 mM aldehyde 143 (data not shown). Given that the linked compound, 1-143, exhibited an IC₅₀ of 25 μM, union of the two subunits rendered a greater than 80-fold enhancement of inhibitory capacity. Since neither compound would have been distinguished if screened separately, these data demonstrate the utility of our library strategy in identifying novel bifunctional inhibitors.

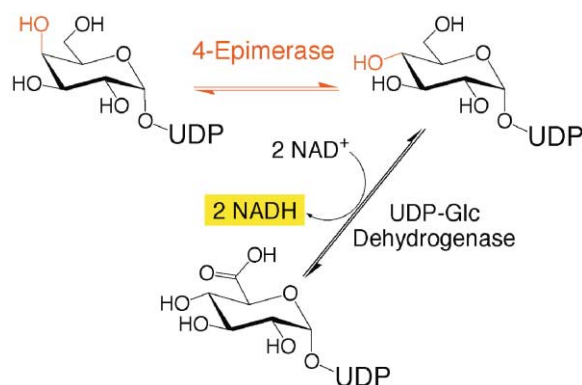


Figure 9. Coupled Enzyme System for the Detection of 4-Epimerase Activity

The assay capitalizes on the 4-epimerase's ability to catalyze the carbohydrate C-4 epimerization in either direction; in this case, UDP-Gal, used as the substrate, is converted to UDP-Glc by the 4-epimerase. UDP-Glc dehydrogenase then oxidizes the product, and simultaneously reduces two molecules of NAD⁺. The production of NADH, and hence 4-epimerase activity, is monitored by the change in absorbance at 340 nm.

Finally, to obtain a refined measurement of the compound's potency and to elucidate its mechanism of inhibition, we performed a K_i measurement. Varying concentrations of UDP-Gal (7.8 μ M–1.0 mM) and 1-143 (10 μ M–80 μ M) were used to obtain a series of double reciprocal plots, as displayed in Figure 14. These data demonstrate that 1-143 is a competitive inhibitor versus UDP-Gal. The apparent K_m of UDP-Gal and K_i of 1-143 were determined to be $140 \pm 7 \mu$ M and $11 \pm 0.6 \mu$ M, respectively. These values compare favorably to those measured for previous, rationally designed substrate analogs of glycosylating enzymes [22–26]. We have noted during handling of 1-143 that the compound is markedly hydrophobic (i.e., it has limited solubility in water), suggesting that its membrane permeability may be superior to previously synthesized, charged substrate analogs. We look forward to the results of ongoing research to test this speculation by monitoring the compound's activity in cultured cells.

Inhibitory Activity of 1-143 against Related Enzymes

The abundance of enzymes acting upon UDP-linked substrates suggests that our uridine-based library could offer chemical tools with which to modulate cellular processes ranging from nucleotide sugar biosynthesis to glycoprotein and glycolipid elongation, to RNA synthesis [40–43]. These enzymes promised both an array of future targets for our uridine-based library and a significant potential risk of unfavorable cross-reactivity with the 4-epimerase inhibitor we had identified. Thus, as a forerunner to cultured cell experiments, it was important to determine if 1-143 showed such unfavorable cross-reactivity *in vitro*. We assessed the compound's selectivity by assaying it against three other enzymes operating on similar substrates. We had already determined that 1-143 was inactive against the UDP-Glc dehydrogenase, which suggested to us that its binding interactions were

fairly specific. To challenge this hypothesis, we assayed the *Streptococcus thermophilus* version of the 4-epimerase, the porcine UDP-GlcNAc/GalNAc pyrophosphorylase, and the bovine β (1-4)galactosyltransferase. We performed IC_{50} measurements for the three enzymes, in each case using substrate concentrations equal to the K_m (bacterial 4-epimerase, UDP-Gal, 100 μ M; pyrophosphorylase, UTP, 200 μ M; galactosyltransferase, UDP-Gal, 100 μ M). As depicted in Figure 15, 1-143 maintained its selective inhibitory behavior. Even at 200 μ M 1-143, the enzymes retained full activity. The data for the bacterial 4-epimerase is perhaps especially noteworthy, as the enzyme is 56% similar to our mammalian target [44]. One difference in substrate specificity exists between the two; the bacterial enzyme operates only on UDP-Gal and not the *N*-acetylated sugar. This may suggest that in its interaction with the human enzyme, compound 1-143 occupies part or all of the pocket normally housing the *N*-acyl group.

Discussion

Glycobiology represents an arena in which chemists can contribute key tools for scientific advance. Because complex carbohydrate structures are inaccessible to direct genetic manipulation—a facile technique for deriving structural information about proteins—chemical tools such as enzyme inhibitors may be the most promising method to modify glycan structures and decode structure-function correlations. We have described a uridine-derived library directed toward a crucial enzyme in O-linked protein glycosylation—the 4-epimerase; we hypothesize that further development of the 4-epimerase inhibitor we identified will produce the first O-linked glycosylation inhibitor for use in cultured cells. In addition, because many glycosylating enzymes act upon UDP-linked substrates, we postulate that this uridine-derived library may serve as a common reservoir from which one could identify inhibitors of other glycosylating enzymes. We anticipate that the documented stability of oxime bonds to physiological pH will imply that hit compounds generated from this library will prove useful in a biological setting [46, 47].

Our screens of the uridine-derived library against the UDP-GlcNAc 4-epimerase provide useful insights into the strategy of library design. Previous workers have capitalized on the strategy of linking two binding elements to enhance their cumulative potency [31, 36]. In these studies, monomer elements were initially screened for binding by NMR, or for inhibitory activity by an ELISA; monomer hits were then joined and their combined potency assessed. The enhancement of potency observed for the dimer versus the most potent monomer ranged from 100- to 625-fold. These values compare favorably with greater than 80-fold inhibitory enhancement we observed upon linking aldehyde 143 with uridine derivative 1. Our approach is distinct in that, since the uridine-derived aspect of the library is held constant, the carbohydrate binding pocket of the enzyme may be targeted specifically for optimal binders. Thus, structural models of the interaction of library hits with the enzyme may be proposed, potentially providing a useful topological map of



The full compound comprises the union of one “R” group depicted below and the indicated uridine derivative above. The bond in bold indicates the point of attachment. These screens used 100 μ M of the enzyme substrate, UDP-Gal, and the same concentration of library compound. The numbers below each R group identify the aldehyde used to make the compound and portray the percent inhibition of enzyme activity observed in the presence of the library compound. Error indicates high/low between duplicate experiments.

that conformational restraints imposed by our current linkers precluded binding by some aldehyde-derived substituents and accounted for the fact that of a 1338 member library, only one compound exhibited greater

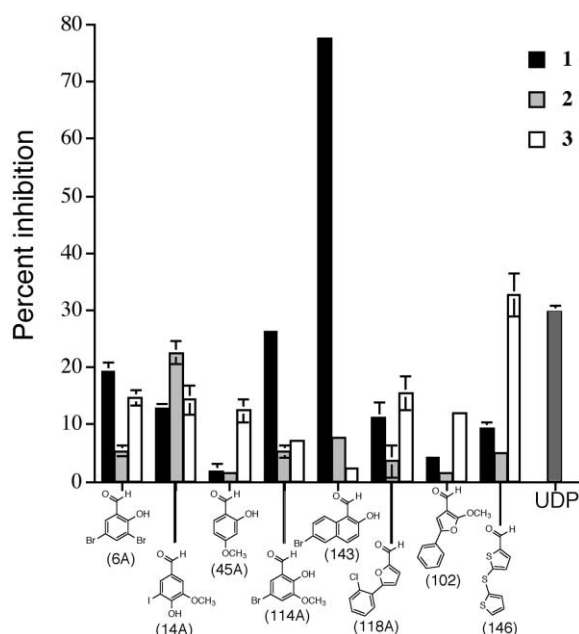


Figure 11. Inhibitory Activity of Selected Library Compounds against the 4-Epimerase

Bars represent the activity of compounds generated by the union of the aldehyde depicted and uridine derivatives 1, 2, or 3. For the assay, 100 μ M each of library compound and substrate (UDP-Gal) were used. Error bars indicate standard deviation ($n = 3$). Aldehyde numbers (in parentheses) correspond with those given in the supporting material.

than 35% inhibition under our screening conditions. Indeed, in the work cited above, both length and flexibility of linkers were found to exert dramatic effects on binding potency, with constrained analogs of hit compounds lagging the activity of their more flexible counterparts by 9.6- to 28-fold [31, 36]. Current efforts in our lab explore this facet of library diversification.

Another consequence of our linker choice may have been the marked specificity of the hit compound we identified for its enzyme target. Of the four additional enzymes tested, none bound 1-143 with measurable potency. If our linker did constrain conformational mobility, this could account for the compound's apparent inability to achieve profitable interactions with the binding sites of other enzymes. Presumably, too, rigidity could become an asset if it locks the relevant compound in a favorable binding orientation. These considerations are now simple speculations, but in future work the consideration of linker flexibility, library binding activity, and inhibitory potency could be further explored.

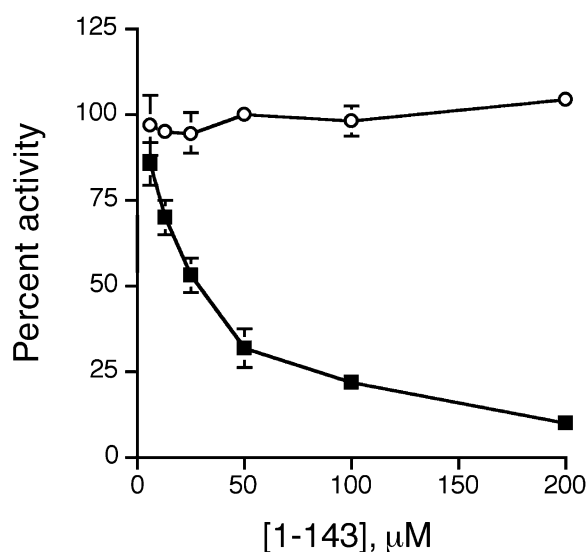


Figure 13. Inhibitory Activity of 1-143 against UDP-Glc Dehydrogenase and Human 4-Epimerase

For each enzyme, substrate concentrations equal to the K_m values were employed (dehydrogenase (\circ), UDP-Glc, 20 μ M; 4-epimerase (\blacksquare), UDP-Gal, 100 μ M). Error bars represent standard deviation ($n = 3$).

Perhaps the most important note about our library strategy was its success at generating a 4-epimerase inhibitor. With a K_i of 11 μ M, 13-fold lower than the measured K_m , compound 1-143 exhibits a binding affinity superior to any neutral inhibitor of a glycosylating enzyme to date. More potent inhibitors incorporate nucleoside phosphates, which are not cell permeable and therefore of limited utility in cellular assays [26]. Structural data may enable second generation enhancement of this inhibitory activity; the 4-epimerase crystal structure has recently been solved, enabling modeling studies of the compound's binding conformation [47]. Furthermore, the compound's current solubility properties encourage speculation that the feat of traversing the cell membrane barrier may be possible. Acetylation of exposed hydroxyl residues could offer means to modulate hydrophobicity were it necessary; deacetylation by cytosolic esterases would be expected to liberate the active compound inside the cell [48].

Significance

Protein glycosylation represents one of the most pervasive and perplexing posttranslational modifications of proteins. A scarcity of chemical tools particularly

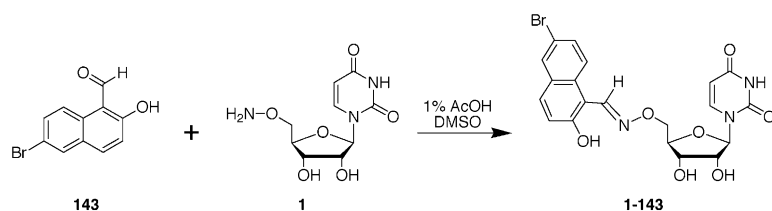


Figure 12. Synthesis of Compound 1-143

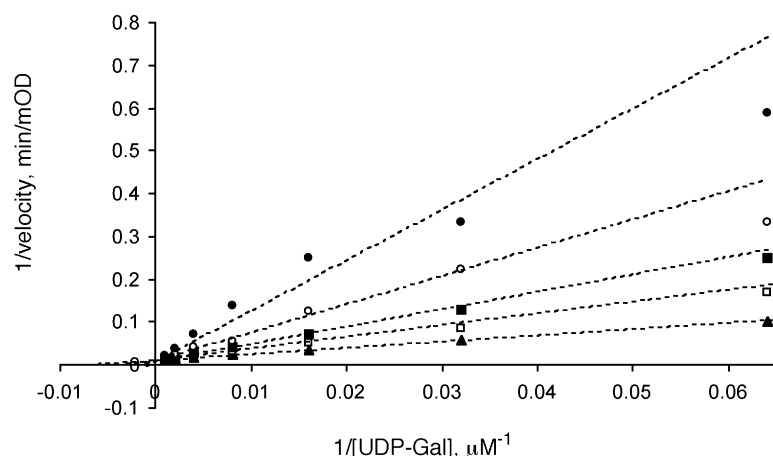


Figure 14. Lineweaver-Burk Analysis of the 4-Epimerase with Inhibitor 1-143

The concentrations of 1-143 used were 0 μM (\blacktriangle), 10 μM (\square), 20 μM (\blacksquare), 40 μM (\circ), and 80 μM (\bullet). Dashed lines represent predicted values based on a competitive inhibition model.

hampers attempts to understand *O*-linked glycosylation. This paper describes a strategy to inhibit the UDP-GlcNAc 4-epimerase, the enzyme responsible for synthesizing UDP-GalNAc, the carbohydrate donor needed to initiate *O*-linked glycosylation. The cornerstone of our approach was a 1338 member library of uridine analogs, from which we identified an inhibitor with a K_i value of 11 μM versus the substrate UDP-Gal. In vitro tests of the compound's potency against a panel of related enzymes confirmed its specificity for the 4-epimerase and suggested that testing of the compound as an inhibitor of *O*-linked glycosylation in cultured cells would be warranted. This work represents a first step toward developing an important

chemical tool for controlling *O*-linked glycosylation; in addition, the library we describe may serve more broadly as a reservoir of potential inhibitors for the many cellular enzymes operating on UDP-linked substrates.

Experimental Procedures

General Methods

RP-HPLC was performed on a Rainin Dynamax SD-200 system using Microsorb and Dynamax C18 reversed-phase columns (analytical: 4.6 mm ID \times 25 cm, 1 ml/min; semipreparative: 10 mm ID \times 25 cm, 4 ml/min) and UV detection (230 nm) was performed with a Rainin Dynamax UV-1 detector. The ^1H and ^{13}C NMR spectra were obtained with Bruker AMX-300 and AMX-400 spectrometers. Chemical shifts are reported in parts per million (ppm) (δ) downfield from tetramethylsilane, and coupling constants are reported in Hz. Mass spectrometry (ESI-MS) was performed on a Hewlett-Packard 5989A mass spectrometer or a Bruker Esquire-LC electrospray ion trap mass spectrometer.

(*t*-BOC-aminoxy)acetic acid was purchased from Fluka (15035). We purchased *tert*-butyl carbazate (*t*-BOC hydrazide) from Aldrich (B9,100-5). Aldehydes 1A-148A were purchased from Aldrich. Aldehydes 1-299 were purchased from ChemDiv (San Diego, CA).

Chemical Synthesis

2',3'-*O*-Isopropylidene Uridine (5)

Uridine (4) (5.0 g, 21 mmol) and TsOH (0.6 g, 3.2 mmol) were added as solids to a flask containing approximately 50 μm sieves and a stir bar. DMF (68 ml) was added, and the solids were allowed to dissolve. 2,2-Dimethoxypropane (10 ml, 82 mmol) was then added and the mixture heated to 40°C. The reaction, monitored by TLC (CHCl_3 :MeOH 10:1; UV visualization, product R_f = 0.42), was judged complete in 1.5 hr. At that time, approximately 1 g (10 scoops) of Amberlyst A-21 ion exchange resin (Aldrich, 21641-0) was added to neutralize the solution; the mixture was stirred for 25 min and then filtered through Celite. The product was purified by silica gel chromatography, eluting with a gradient of CHCl_3 :MeOH to yield 5.8 g (89%) of white solid. ^1H NMR (500 MHz, CD_3OD) δ 1.36 (s, 3H), 1.56 (s, 3H), 3.73 (dd, 1H, J = 4.5, 11.9 Hz), 3.79 (dd, 1H, J = 3.6, 11.9 Hz), 4.21–4.23 (m, 1H), 4.83 (dd, 1H, J = 3.4, 6.3 Hz), 4.92 (dd, 1H, J = 2.8, 6.3 Hz), 5.70 (d, 1H, J = 8.0 Hz), 5.88 (d, 1H, J = 2.8 Hz), 7.84 (d, 1H, J = 8.1 Hz). ^{13}C NMR (100 MHz, CD_3OD) δ 25.53, 27.54, 63.05, 82.21, 85.81, 88.37, 94.10, 102.61, 115.10, 143.87, 152.07, 166.21. Analytical calculated for $\text{C}_{12}\text{H}_{16}\text{N}_2\text{O}_6$: C, 50.70; H, 5.67; N, 9.85. Found: C, 50.42; H, 5.79; N, 9.79.

2',3'-*O*-Isopropylidene-5'-*O*-Toluenesulfonyluridine (6)

2',3'-*O*-Isopropylidene uridine (5) (4.1 g, 14 mmol) was suspended in CH_2Cl_2 (58 ml); the subsequent addition of pyridine (11.7 ml, 144 mmol) caused compound 5 to dissolve completely. After addition of Ts_2O (7.5 g, 23 mmol), the solution turned yellow and warmed

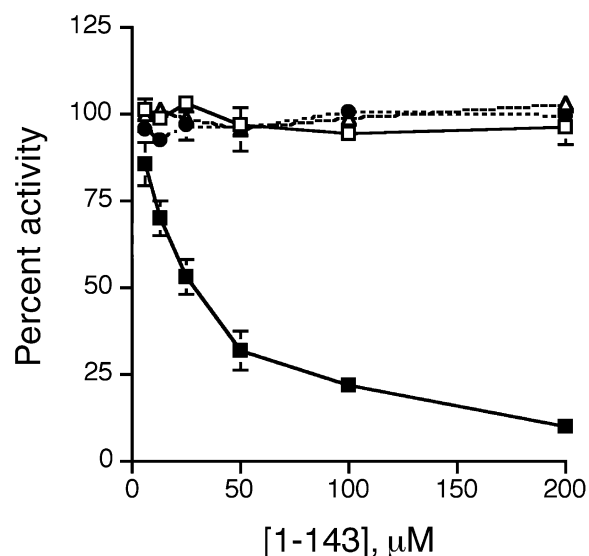


Figure 15. Selectivity of Inhibition by 1-143 for the Human 4-Epimerase

Inhibitory activity of 1-143 against UDP-GlcNAc/GalNAc pyrophosphorylase (\bullet), bacterial 4-epimerase (\square), β (1-4)galactosyltransferase (\triangle), and human 4-epimerase (\blacksquare). For each enzyme, substrate concentrations equal to the K_m values were employed (bacterial 4-epimerase, UDP-Gal, 100 μM ; pyrophosphorylase, UTP, 200 μM ; galactosyltransferase, UDP-Gal, 100 μM ; human 4-epimerase, UDP-Gal, 100 μM). Error bars represent standard deviation (n = 3).

slightly. The reaction was heated at reflux for 2 hr, at which point it was judged complete by TLC (CHCl_3 :MeOH, 10:1, UV visualization). The reaction was diluted with 250 ml of CHCl_3 and washed with 0.5 M HCl (5×100 ml) and saturated NaHCO_3 (2×100 ml). After drying over Na_2SO_4 , the organic layer was filtered, concentrated in vacuo, and coevaporated with toluene until the crude product was a yellow solid. Purification by silica gel chromatography eluting with a gradient of CHCl_3 :MeOH yielded 6.2 g (98%) of an off-white solid. ^1H NMR (500 MHz, CDCl_3) δ 1.30 (s, 3H), 1.51 (s, 3H), 2.40 (s, 3H), 4.22–4.28 (m, 2H), 4.30–4.33 (m, 1H), 4.77 (dd, 1H, $J = 3.8, 6.4$ Hz), 4.94 (dd, 1H, $J = 1.9, 6.4$ Hz), 5.62 (d, 1H, $J = 1.9$ Hz), 5.70 (app d, 1H, $J = 8.0$ Hz), 7.24 (d, 1H, $J = 8.1$ Hz), 7.30 (d, 2H, $J = 8.0$ Hz), 7.73 (d, 2H, $J = 8.3$ Hz), 9.96 (app s, 1H). ^{13}C NMR (100 MHz, CDCl_3) δ 21.72, 25.22, 27.06, 69.53, 80.92, 84.40, 85.24, 95.04, 102.71, 114.66, 128.02, 129.95, 132.52, 142.67, 145.34, 150.20, 163.79.

2',3'-O-Isopropylidene-5'-O-Succinimidyluridine (7)

2',3'-O-Isopropylidene-5'-O-toluenesulfonyluridine (6) (7.0 g, 16 mmol) and *N*-hydroxysuccinimide (5.5 g, 48 mmol) were dissolved in DMF (40 ml); DIEA (14 ml, 80 mmol) was added, and the solution was stirred at 40°C for 6 hr. At this time, the reaction was judged complete by TLC (CHCl_3 :MeOH, 6:1, UV visualization). The solution, concentrated in vacuo, was coevaporated with toluene to ensure removal of the DMF. The crude mixture was dissolved in 600 ml of CHCl_3 and washed with 0.5 M HCl (3×100 ml) and saturated NaHCO_3 (1×100 ml). Numerous back-extractions of the aqueous layers were required to rescue the product. The combined organic layers were dried over Na_2SO_4 , filtered, and concentrated in vacuo. Purification was accomplished by silica gel chromatography eluting with a gradient of CHCl_3 :MeOH to yield 4.6 g (76%) of an off-white solid. ^1H NMR (500 MHz, CD_3OD) δ 1.36 (s, 3H), 1.55 (s, 3H), 2.68 (s, 4H), 4.33 (d, 2H, $J = 4.4$ Hz), 4.45–4.48 (m, 1H), 4.97 (dd, 1H, $J = 2.4, 6.3$ Hz), 4.99 (dd, 1H, $J = 3.0, 6.3$ Hz), 5.69 (d, 1H, $J = 8.0$ Hz), 5.84 (d, 1H, $J = 2.4$ Hz), 7.84 (d, 1H, $J = 8.1$ Hz). ^{13}C NMR (100 MHz, CD_3OD) δ 25.52, 26.47, 27.46, 77.52, 82.42, 85.64, 85.99, 95.11, 102.82, 115.27, 144.20, 152.00, 166.14, 173.68. HRMS calculated for $\text{C}_{16}\text{H}_{20}\text{N}_3\text{O}_8$ ($M + \text{H}^+$), 382.1250; found, 382.1240.

5'-O-Succinimidyluridine (8)

2',3'-O-Isopropylidene-5'-O-succinimidyluridine (7) (3.6 g, 9.4 mmol) was dissolved in 50 ml of 90% TFA in H_2O . The reaction, monitored by TLC (CHCl_3 :MeOH, 10:1, UV visualization) was complete within 25 min. The solution was concentrated in vacuo, with subsequent coevaporation with toluene to remove residual solvent. Purification by silica gel chromatography, eluting with a gradient of CHCl_3 :MeOH, yielded 3.1 g (97%) of a hygroscopic white solid. ^1H NMR (500 MHz, d_6 -DMSO) δ 2.61 (s, 4H), 4.03–4.09 (m, 3H), 4.18 (dd, 1H, $J = 2.6, 10.6$ Hz), 4.25 (dd, 1H, $J = 4.9, 10.6$ Hz), 5.33 (d, 1H, $J = 4.3$ Hz), 5.50 (d, 1H, $J = 5.1$ Hz), 5.61 (dd, 1H, $J = 2.2, 8.1$ Hz), 5.78 (d, 1H, $J = 5.0$ Hz), 7.78 (d, 1H, $J = 8.1$ Hz), 11.36 (d, 1H, $J = 1.9$ Hz). ^{13}C NMR (500 MHz, d_6 -DMSO) δ 25.47, 69.96, 72.87, 76.23, 81.52, 88.25, 101.98, 140.91, 150.70, 163.05, 171.91. Analytical calculated for $\text{C}_{13}\text{H}_{15}\text{N}_3\text{O}_8 + \text{H}_2\text{O}$: C, 43.46; H, 4.77; N, 11.70. Found: C, 43.32; H, 4.68; N, 11.57.

5'-Aminoxyuridine (1)

5'-O-Succinimidyluridine (8) (3.0 g, 8.8 mmol) was dissolved in a 2:1 mixture of 40% $\text{MeNH}_2/\text{H}_2\text{O}$ and MeOH (60 ml total) and heated to reflux. As monitored by TLC (CHCl_3 :MeOH, 2:1, UV visualization), the reaction was complete within 2 hr. The solution was concentrated in vacuo to provide an off-white solid, which was redissolved in H_2O with trace CH_3CN added to aid dissolution. The product was purified by HPLC on a preparative aminopropyl silica gel column (Rainin, 21.4 mm diameter, 25 cm length, 60 Å pore) eluting with a gradient of $\text{CH}_3\text{CN}:\text{H}_2\text{O}$ (100% to 50% CH_3CN over 45 min). Lyophilization yielded 2.3 g (59%) of a fluffy white solid. ^1H NMR (500 MHz, d_6 -DMSO) δ 3.68 (dd, 1H, $J = 5.1, 11.2$ Hz), 3.74 (dd, 1H, $J = 3.4, 11.2$ Hz), 3.91–3.92 (m, 1H), 3.95–3.97 (m, 1H), 4.02 (app dd, 1H, $J = 5.2, 10.5$ Hz), 5.21 (d, 1H, $J = 4.5$ Hz), 5.42 (d, 1H, $J = 5.6$ Hz), 5.65 (dd, 1H, $J = 0.2, 8.1$ Hz), 5.75 (d, 1H, $J = 5.5$ Hz), 6.18 (s, 2H), 7.68 (d, 1H, $J = 8.1$ Hz), 11.33 (s, 1H). ^{13}C NMR (500 MHz, d_6 -DMSO) δ 70.26, 72.99, 75.40, 82.16, 88.08, 102.06, 140.89, 150.76, 163.14. HRMS calculated for $\text{C}_9\text{H}_{13}\text{N}_3\text{O}_6$ ($M + \text{H}^+$), 260.0883; found, 260.0884.

5'-Azido-5'-Deoxy-2',3'-O-Isopropylidene Uridine (9)

2',3'-O-Isopropylidene-5'-O-toluenesulfonyluridine (3.20) (6.0 g, 14 mmol) was dissolved in DMF (34 ml). LiN_3 (3.4 g, 68 mmol) [49] was added; this compound never entirely dissolved. The reaction was

heated at 45°C overnight; as monitored by TLC (hexanes:ethyl acetate, 1:1.5, UV visualization), it was judged complete the following morning. Because the azido-uridine product (9) was unreactive to all reduction conditions tested, including Staudinger conditions, it was fruitless to attempt to monitor the reaction using triphenylphosphine/ninhydrin staining. The solution was concentrated in vacuo and coevaporated with toluene several times to remove residual DMF. Because the product partitioned between aqueous and organic layers, the crude mixture was purified directly by silica gel chromatography using a gradient of CHCl_3 :MeOH to yield 4.4 g (98%) of a hygroscopic off-white solid. ^1H NMR (500 MHz, CDCl_3) δ 1.32 (s, 3H), 1.53 (s, 3H), 3.59–3.61 (m, 2H), 4.19–4.21 (m, 1H), 4.80 (dd, 1H, $J = 4.2, 6.5$ Hz), 4.99 (dd, 1H, $J = 2.1, 6.5$ Hz), 5.64 (d, 1H, $J = 2.1$ Hz), 5.74 (d, 1H, $J = 8.0$ Hz), 7.30 (d, 1H, $J = 8.1$ Hz), 10.18 (s, 1H). ^{13}C NMR (500 MHz, CDCl_3) δ 25.26, 27.12, 52.38, 81.60, 84.36, 85.96, 94.91, 102.86, 114.78, 142.75, 150.30, 163.91.

5'-Azido-5'-Deoxy Uridine (10)

To a flask containing 5'-azido-5'-deoxy-2',3'-O-isopropylidene uridine (9) (3.2 g, 10 mmol), 60 ml of 90% TFA in water was added. The reaction, monitored by TLC (CHCl_3 :MeOH, 6:1, UV visualization), was complete within 20 min. At that time, the solution was concentrated in vacuo, with repeated coevaporation with toluene to remove residual water. The product was purified by silica gel chromatography eluting with a gradient of CHCl_3 :MeOH to yield 2.7 g (96%) of a white glass. ^1H NMR (500 MHz, CD_3OD) δ 3.60 (dd, 1H, $J = 4.8, 13.4$ Hz), 3.69 (dd, 1H, $J = 3.2, 13.4$ Hz), 4.04–4.08 (m, 1H), 4.09–4.11 (m, 1H), 4.21–4.23 (m, 1H), 5.74 (d, 1H, $J = 8.1$ Hz), 5.84 (d, 1H, $J = 4.3$ Hz), 7.72 (d, 1H, $J = 8.1$ Hz). ^{13}C NMR (500 MHz, CD_3OD) δ 53.05, 71.70, 74.79, 83.73, 91.72, 103.01, 142.63, 152.25, 166.07. Analytical calculated for $\text{C}_9\text{H}_{11}\text{N}_5\text{O}_5$: C, 40.15; H, 4.12; N, 26.01. Found: C, 40.12; H, 4.37; N, 25.90.

5'-Amino-5'-Deoxy Uridine (11)

5'-Azido-5'-deoxy uridine (10) (2.5 g, 9.3 mmol) was suspended in MeOH (60 ml) and 10% Pd/C (0.5 g) was added. While the mixture was stirred at room temperature, H_2 gas was bubbled through the solvent; the starting material gradually dissolved as the reaction progressed. As monitored by TLC (CHCl_3 :MeOH, 2:1, UV and ninhydrin visualization), the reaction was complete in 3 hr. The solution, filtered through Celite, was concentrated in vacuo to yield 2.2 g (98%) of product judged sufficiently clean by ^1H NMR to carry on without further purification. ^1H NMR (500 MHz, d_6 -DMSO) δ 2.74 (dd, 1H, $J = 5.4, 13.6$ Hz), 2.79 (dd, 1H, $J = 4.5, 13.6$ Hz), 3.74–3.76 (m, 1H), 3.91 (m, 1H), 4.06 (app t, 1H, $J = 5.5$ Hz), 5.63 (d, 1H, $J = 8.0$ Hz), 5.74 (d, 1H, $J = 5.6$ Hz), 7.85 (d, 1H, $J = 8.1$ Hz). ^{13}C NMR (500 MHz, d_6 -DMSO) δ 43.16, 70.40, 73.02, 85.01, 88.07, 101.95, 141.43, 150.85, 163.22. HRMS calculated for $\text{C}_9\text{H}_{14}\text{N}_3\text{O}_5$ ($M + \text{H}^+$), 244.0933; found, 244.0939.

Compound 12

5'-Amino-5'-deoxy uridine (11) (2.0 g, 8.2 mmol), HOBt (1.9 g, 12 mmol), and (*t*-BOC-aminoxy)acetic acid (3.1 g, 16 mmol) were dissolved together in DMF (33 ml) and stirred at room temperature for 30 min. EDC (2.4 g, 12 mmol) was then added. The mixture was stirred at room temperature under Ar for approximately 14 hr, at which time the reaction appeared complete by TLC (CHCl_3 :MeOH, 2:1, UV visualization). The solution was concentrated in vacuo, with repeated coevaporation with toluene to remove residual DMF. The crude product was purified by silica gel chromatography eluting with a gradient of CHCl_3 :MeOH to yield 3.1 g (91%) of an off-white solid. ^1H NMR (500 MHz, d_6 -DMSO) δ 1.39 (s, 9H), 3.29–3.34 (m, 1H), 3.47–3.52 (m, 1H), 3.81–3.88 (m, 2H), 4.06 (app q, 1H, $J = 5.5$ Hz), 4.18 (s, 2H), 5.19 (d, 1H, $J = 5.2$ Hz), 5.40 (d, 1H, $J = 5.7$ Hz), 5.63 (dd, 1H, $J = 2.2, 8.1$ Hz), 5.73 (d, 1H, $J = 5.6$ Hz), 7.66 (d, 1H, $J = 8.1$ Hz), 8.17 (app s, 1H), 10.28 (s, 1H), 11.35 (d, 1H, $J = 2.0$ Hz). ^{13}C NMR (500 MHz, d_6 -DMSO) δ 27.93, 40.61, 70.81, 72.51, 74.73, 80.72, 82.26, 88.30, 102.00, 141.22, 150.73, 156.92, 163.07, 168.29. Analytical calculated for $\text{C}_{16}\text{H}_{24}\text{N}_4\text{O}_9 + \text{H}_2\text{O}$: C, 44.24; H, 6.03; N, 12.90. Found: C, 44.09; H, 5.89; N, 12.93.

Compound 2

Compound 12 (3.4 g, 8.2 mmol) was dissolved in a solution of 40% TFA in CH_2Cl_2 (150 ml). The presence of TFA complicated the monitoring of the reaction by TLC (CHCl_3 :MeOH, 2:1, UV visualization), but the reaction progress was rapid and deprotection was definitively complete within 45 min. The reaction was stopped by concentration in vacuo; coevaporation with toluene ensured removal of the TFA.

The crude product was purified by HPLC on a preparative aminopropyl silica gel column (Rainin, 21.4 mm diameter, 25 cm length, 60 Å pore) eluting with a gradient of $\text{CH}_3\text{CN}:\text{H}_2\text{O}$. Lyophilization yielded 1.2 g (45%) of a fluffy white solid. ^1H NMR (500 MHz, d_6 -DMSO) δ 3.29–3.34 (m, 1H), 3.42–3.47 (m, 1H), 3.84–3.87 (m, 1H), 3.90–3.92 (m, 1H), 3.97 (s, 1H), 4.07 (app t, 1H, $J = 5.5$ Hz), 5.19 (s, 1H), 5.39 (s, 1H), 5.64 (d, 1H, $J = 8.0$ Hz), 5.72 (d, 1H, $J = 5.7$ Hz), 6.34 (s, 2H), 7.67 (d, 1H, $J = 8.1$ Hz), 7.94 (app t, 1H, $J = 6.0$ Hz), 11.28 (s, 1H). ^{13}C NMR (500 MHz, d_6 -DMSO) δ 40.53, 70.92, 72.57, 74.41, 82.57, 88.44, 102.10, 141.50, 150.88, 163.27, 170.38. Analytical calculated for $\text{C}_{11}\text{H}_{16}\text{N}_4\text{O}_7$: C, 41.77; H, 5.10; N, 17.72. Found: C, 41.33; H, 5.32; N, 17.40.

4-Chlorosulfonyl Benzoic Acid Methyl Ester (13)

4-Chlorosulfonyl benzoic acid (5.0 g, 23 mmol) was suspended in a mixture of thionyl chloride (20 ml) and dichloroethane (10 ml), the latter added to enhance the solubility of the starting material. The mixture was heated to reflux; gradually, the starting material dissolved during heating. The reaction was heated at reflux for 1 hr following complete dissolution of the starting material, at which time it was concentrated in vacuo to a light-brown solid, presumably the crude intermediate 4-chlorosulfonyl benzoyl chloride. This material was chilled on ice for several minutes; ice-cold MeOH (40 ml) was then added and the mixture stirred on ice for 5 min, which left most but not all of the solid dissolved. The reaction was then removed from ice and stirred at room temperature for 10 min, during which time a white precipitate was formed. Addition of ice-cold H_2O (40 ml) yielded copious precipitation. The solid product was filtered from the solvent, washed with additional ice-cold H_2O , and dried under vacuum to yield 4.6 g (86%) of white solid judged >95% pure by ^1H NMR [50]. ^1H NMR (500 MHz, CDCl_3) δ 3.97 (s, 3H), 8.24 (d, 2H, $J = 2.0$ Hz), 8.26 (d, 2H, $J = 1.9$ Hz). ^{13}C NMR (500 MHz, CDCl_3) δ 52.91, 127.00, 130.79, 136.01, 147.33, 164.83.

Compound 14

5'-Amino-5'-deoxy uridine (11) (2.0 g, 8.2 mmol) was dissolved in DMF (33 ml). TEA (2.3 ml, 16 mmol) and 4-chlorosulfonyl benzoic acid methyl ester (13) (2.3 g, 9.8 mmol) were added, yielding a pale yellow mixture in which some undissolved sulfonyl chloride was suspended. The reaction was stirred at room temperature overnight. As monitored by TLC ($\text{CHCl}_3:\text{MeOH}$, 2:1, UV visualization), the reaction was judged complete the following morning. The coupled product was insoluble in most solvents and was most efficiently purified by precipitation from MeOH in three successive batches, which yielded 2.5 g (70%) of white solid judged >95% pure by ^1H NMR. ^1H NMR (500 MHz, d_6 -DMSO) δ 2.97–3.02 (m, 1H), 3.11–3.15 (m, 1H), 3.74–3.77 (m, 1H), 3.85–3.88 (m, 1H), 3.89 (s, 3H), 4.04 (app q, 1H, $J = 5.7$ Hz), 5.20 (d, 1H, $J = 5.3$ Hz), 5.40 (d, 1H, $J = 5.8$ Hz), 5.60 (dd, 1H, $J = 1.9, 8.0$ Hz), 5.68 (d, 1H, $J = 5.9$ Hz), 7.61 (d, 1H, $J = 8.1$ Hz), 7.92–7.95 (m, 2H), 8.11–8.15 (m, 2H), 11.34 (d, 1H, $J = 1.6$ Hz). ^{13}C NMR (500 MHz, d_6 -DMSO) δ 44.66, 52.64, 70.43, 72.10, 82.41, 88.18, 101.95, 126.93, 130.02, 132.86, 141.39, 144.65, 150.71, 163.01, 165.21. HRMS calculated for $\text{C}_{17}\text{H}_{20}\text{N}_5\text{O}_9\text{S}_1$ ($\text{M} + \text{H}^+$), 442.0920; found, 442.0920.

Compound 15

Compound 14 (1.6 g, 3.6 mmol) was suspended in a 3:1 mixture of $\text{MeOH}:\text{H}_2\text{O}$ (36 ml total) and stirred on ice for 15 min. LiOH (0.43 g, 18 mmol) was added, causing the uridine derivative to dissolve; the solution was stirred on ice overnight. The following morning, the reaction was judged complete by TLC analysis ($\text{CHCl}_3:\text{MeOH}$ 2:1, UV visualization). Approximately 1 g of Amberlite IRC-50 resin was added to neutralize the basic solution, and the mixture was stirred at room temperature for 30 min. The solution was removed from the resin by filtration and the solution concentrated in vacuo; the crude product was taken on without purification to the next reaction. This intermediate was dissolved in anhydrous DMF (18 ml), which was followed by the successive additions of HOBt (0.83 g, 5.4 mmol) and *t*-BOC hydrazide (0.95 g, 7.2 mmol). The resultant solution was stirred at room temperature under Ar for 15 min. EDC (1.0 g, 5.4 mmol) was then added and the reaction stirred at room temperature under Ar overnight. The following morning, the reaction was judged complete by TLC analysis ($\text{CHCl}_3:\text{MeOH}$, 2:1, UV visualization); concentration in vacuo, followed by coevaporation with toluene, was performed to remove all solvent. Purification was accomplished by silica gel chromatography using a gradient of $\text{CHCl}_3:\text{MeOH}$ to yield 1.9 g (97% over two steps) of white solid. It should be noted that

HOBt often coeluted with the product during purification; most often the product was carried forward without further separating this minor impurity. ^1H NMR (500 MHz, MeOD) δ 3.16 (dd, 1H, $J = 5.7, 14.1$ Hz), 3.24–3.31 (m, 2H), 3.91–3.94 (m, 1H), 4.07 (app t, 1H, $J = 5.5$ Hz), 4.19–4.22 (m, 1H), 5.70 (d, 1H, $J = 8.0$ Hz), 5.73 (d, 1H, $J = 4.8$ Hz), 7.65 (d, 1H, $J = 8.1$ Hz), 7.95 (d, 2H, $J = 8.4$ Hz), 8.00 (d, 2H, $J = 8.2$ Hz). ^{13}C NMR (500 MHz, MeOD) δ 28.45, 28.55, 44.91, 45.56, 71.86, 74.47, 82.08, 83.87, 91.92, 102.94, 128.19, 129.46, 143.18, 144.98, 152.35, 166.18, 168.23. HRMS calculated for $\text{C}_{21}\text{H}_{27}\text{N}_5\text{O}_{10}\text{S}_1$ ($\text{M} + \text{H}^+$), 542.1557, found 542.1554.

Compound 3

Compound 15 (2.1 g, 3.9 mmol) was dissolved in a solution of 40% TFA in CH_2Cl_2 (60 ml). Bubbles of CO_2 were observed upon addition of solvent. The reaction was stirred at room temperature for 2 hr, at which time it appeared to be complete by TLC analysis ($\text{CHCl}_3:\text{MeOH}$, 2:1, UV visualization). The reaction was concentrated in vacuo, with subsequent rounds of coevaporation with toluene to ensure removal of the TFA. The crude product, an off-white glass, was dissolved in MeOH and purified by HPLC on a preparative aminopropyl silica gel column (Rainin, 21.4 mm diameter, 25 cm length, 60 Å pore), eluting with a gradient of $\text{CH}_3\text{CN}:\text{H}_2\text{O}$ (100% to 50% CH_3CN over 45 min). Lyophilization yielded 0.94 g (55%) of a fluffy white solid. ^1H NMR (500 MHz, d_6 -DMSO) δ 2.95 (dd, 1H, $J = 6.5, 13.8$ Hz), 3.09 (dd, 1H, $J = 4.9, 13.7$ Hz), 3.76–3.79 (m, 1H), 3.87–3.89 (m, 1H), 4.06 (app t, 1H, $J = 5.5$), 4.58 (s, 2H), 5.25 (s, 1H), 5.45 (s, 1H), 5.61 (d, 1H, $J = 8.1$ Hz), 5.71 (d, 1H, $J = 6.0$ Hz), 7.64 (d, 1H, $J = 8.1$ Hz), 7.86 (app d, 2H, $J = 8.7$ Hz), 7.98 (app d, 2H, $J = 8.7$ Hz), 10.01 (s, 1H). ^{13}C NMR (500 MHz, d_6 -DMSO) δ 44.65, 70.47, 72.13, 82.56, 88.15, 101.96, 126.55, 127.90, 136.80, 141.42, 142.65, 150.76, 157.89, 158.14, 163.07, 164.59. HRMS calculated for $\text{C}_{16}\text{H}_{20}\text{N}_5\text{O}_8\text{S}_1$ ($\text{M} + \text{H}^+$), 442.1033; found 442.1026.

Compound 1-143

Aldehyde 143 (15 mg, 0.060 mmol) and uridine derivative 1 (20 mg, 0.077 mmol) were combined in 1% AcOH/DMSO (600 μL), vortexed, and incubated at room temperature in the dark overnight. The reaction, as monitored by RP-HPLC, was complete the next day. Compound 1-143 was purified by RP-HPLC using a gradient of $\text{CH}_3\text{CN}/\text{NH}_4\text{OAc}$ (25 mM, pH 7.0); lyophilization yielded 19 mg (65%) of product. As described in the text, the *E* isomer was invariably mixed with a small percentage of *Z* isomer. For the assays described herein, that mixture—as estimated by ^1H NMR analysis of oxime proton resonances—was 96% *E* (oxime resonance at 8.94 ppm) to 4% *Z* (oxime resonance at 7.90 ppm). ^1H NMR of *E* isomer (500 MHz, d_6 -DMSO): δ 4.05–4.06 (m, 1H), 4.10–4.14 (m, 2H), 4.40 (dd, 1H, $J = 5.5, 12.2$ Hz), 4.47 (dd, 1H, $J = 3.5, 12.3$ Hz), 5.30 (app s, 1H), 5.49 (d, 1H, $J = 5.5$ Hz), 5.56 (d, 1H, $J = 8.1$ Hz), 5.80 (d, 1H, $J = 5.1$ Hz), 7.26 (d, 1H, $J = 9.0$ Hz), 7.62 (dd, 1H, $J = 2.2, 9.2$ Hz), 7.72 (d, 1H, $J = 8.1$ Hz), 7.88 (d, 1H, $J = 9.0$ Hz), 8.13 (d, 1H, $J = 2.1$ Hz), 8.65 (d, 1H, $J = 9.2$ Hz), 8.94 (s, 1H), 11.34 (s, 1H). ^{13}C NMR (500 MHz, d_6 -DMSO): δ 69.89, 72.70, 73.87, 82.17, 88.45, 101.87, 108.72, 116.19, 119.35, 126.59, 129.47, 129.80, 130.27, 130.38, 131.62, 140.80, 147.11, 150.65, 156.66, 162.99. HRMS calculated for $\text{C}_{20}\text{H}_{20}\text{Br}_1\text{N}_5\text{O}_7$ ($\text{M} + \text{H}^+$), 494.0386; found, 494.0383.

Library Coupling Reactions

For aldehydes 1A-148A, since quantities permitted, the aldehydes were dissolved in DMSO at a concentration of 0.2 M. These solutions were incubated at room temperature for 3 days to maximize dissolution of the aldehydes. Some compounds never fully dissolved (38A, 43A, 101A, 106A, 107A, 109A, 110A, 112A); in these cases, the suspension was used for the coupling reaction, and it should be assumed that the concentrations of these aldehydes have been overestimated. Aldehyde 113A was not used for library couplings, as it was too volatile to handle accurately. Uridine derivatives 1, 2, and 3 were dissolved in 2% AcOH/DMSO (vol/vol) at a concentration of 0.22 M. Equal volumes (50 μL each) of aldehyde and uridine derivative were combined, vortexed, and incubated at room temperature in the dark for 4 days. At this point, the couplings were assumed to be complete, and the library solutions were stored at -20°C . Aliquots of these 100 mM solutions were diluted 50-fold with DMSO, to a final concentration of 2 mM, for use in library screening.

The efficiencies of 33 of these library couplings (the reactions of uridine derivatives 1, 2, and 3 with 11 aldehydes each, as depicted

in Table 1) were quantitated by ^1H NMR. Identical conditions to those just described were used, except that d_6 -DMSO was substituted as the solvent, and a suitable volume was employed to allow ^1H NMR readings. The product yield was calculated by comparing the relative intensities of the product oxime or hydrazone proton resonance (typically found between 7.0 and 9.5 ppm) with that of the starting material aldehyde proton resonance (typically found between 8.5 and 11.0 ppm). The identities of the coupled products were confirmed by electrospray mass spectrometry.

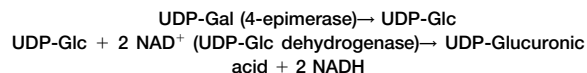
Aldehydes 1–299 were purchased as 20 mM solutions in DMSO. In some cases, the compounds were not fully soluble at this concentration; if so, the suspension was used. Uridine derivatives 1, 2, and 3 were dissolved in 0.2% AcOH/DMSO (vol/vol) at a concentration of 22 mM. Equal volumes (25 μL each) of aldehyde and uridine derivative were combined, vortexed, and incubated at room temperature in the dark for 4 days. At this point, the couplings were assumed to be complete, and the library solutions stored at -20°C . Aliquots of these 10 mM solutions were diluted 5-fold with DMSO, to a final concentration of 2 mM, for use in library screening.

The efficiencies of 99 of these library couplings (the reactions of uridine derivatives 1, 2, and 3 with 33 aldehydes each, as depicted in Table 1) were quantitated by RP-HPLC. A gradient of $\text{CH}_3\text{CN}/\text{NH}_4\text{OAc}$ (25 mM, pH 7.0) (10%–80% NH_4OAc over 8 min) was used on an analytical C18 column (Rainin, 4.6 mm diameter, 25 cm length, 100 Å pore); absorbance was monitored at 254 nm. Standard curves of each uridine derivative were measured to correlate the absorbance intensity with the concentration of uridine analog. To calculate library coupling yields, we exposed an aliquot of the reaction mixture to the same RP-HPLC conditions, and the intensity of the peak corresponding to the uridine analog was compared to the standard curves generated previously. The percent diminution of the uridine starting material was assumed to represent a coincident percent accumulation of product. This method of yield estimation demanded the presence of a solitary product; in those cases where multiple product peaks were observed, this method was judged inappropriate to estimate yields. The identities of the coupled products were confirmed by electrospray mass spectrometry.

Spectrophotometric Assay for 4-Epimerase Activity

General Conditions

Activity of the 4-epimerase was monitored using a coupled enzyme assay as summarized below:



The production of NADH, and hence the activity of the 4-epimerase, was monitored by measuring the absorbance at 340 nm. Assays were performed in half-area 96-well plates (Corning costar 3696) with 100 μL per well unless reagents were limiting, in which case 50 μL per well was used. Protocols that follow assume 100 μL per well. For library screening, each well contained assay reagents in the following final concentrations: 100 μM library compound; 100 μM UDP-Gal (Calbiochem 670111); 0.1 mU bacterial 4-epimerase (Calbiochem 670112) or 0.05 mU human 4-epimerase (purification from yeast described below; note that less human enzyme was used simply to conserve enzyme); 16 mU UDP-Glc dehydrogenase (Calbiochem 670121); 1.25 mM β -NAD $^+$ (Sigma N1511); 125 mM potassium bicinate (pH 8.5) (Sigma B3876).

Library Screening

For library screening, 5 μL of each of library compound or control (0.02% AcOH/DMSO solution) and UDP-Gal (H_2O solution) were aliquoted to each well. An enzyme cocktail comprising appropriate concentrations of the remaining reagents was assembled on ice; this cocktail was incubated at room temperature for 10 min prior to assay initiation to allow its temperature to equilibrate. The assay was initiated by dispensing 90 μL of cocktail per well using a multi-channel pipettor. Absorbance at 340 nm was monitored on a Molecular Devices SpectraMAX190 microplate reader for 5 min, with readings every 3 s. Note that to achieve readings of this frequency, only three columns of the plate could be read at once. Initial rates of enzymatic reactions were determined using the SoftMAX Pro software that accompanies the SpectraMAX190 machine. Percent inhi-

bition was calculated using the following formula: % inhibition = $100 - ((\text{experimental rate}/\text{control rate}) \times 100)$. The control rate represented the average of quadruplicate samples containing 5 μL of DMSO in place of 5 μL of library compound dissolved in DMSO. For initial library screening, the compounds were screened in duplicate and error depicted by high/low values.

Because this assay monitors light absorption, results were in some cases complicated by the spectrophotometric properties of the library compounds themselves. Specifically, we observed that the absorbance of the library compounds sometimes changed upon incubation with enzyme cocktail, irrespective of the presence of the enzyme substrate, UDP-Gal. This led to the identification of false positives in the initial screens. To clarify the activity of the library compounds, the assay protocol was altered slightly in rescreening and IC $_{50}$ experiments. All reagents were used in the final concentrations described above. In the revised format, only 5 μL of library compound, and no UDP-Gal, was aliquoted into the microplate. The remaining reagents were divided into two cocktails, both assembled on ice: (A) contained 4-epimerase, UDP-Glc dehydrogenase, β -NAD $^+$, and potassium bicinate; and (B) contained UDP-Gal, β -NAD $^+$, and potassium bicinate. Cocktail A was incubated at room temperature for 5 min prior to assay initiation, and then 45 μL per well was dispensed with a multichannel pipettor. Absorbance at 340 nm was monitored for 5–10 min, until those readings achieved a stable baseline. Cocktail B, which was incubated at room temperature for 10 min prior to use, was then dispensed at 50 μL per well; this initiated the enzymatic reaction. As previously, absorbance at 340 nm was monitored for 5 min, and initial rates were calculated and compared to a control exposed to only DMSO.

K $_i$ Measurement

UDP-Gal was aliquoted to a 96-well plate (10 μL per well of $10 \times$ stock solutions designed to yield final concentrations ranging from 7.6×10^{-6} M to 1.0×10^{-3} M). A suitable amount of compound 1–143 was added to five separate batches of enzyme cocktail so as to yield final concentrations in the wells of 0, 10, 20, 40, and 80×10^{-6} M 1–143. The enzyme/1–143 cocktail was incubated at room temperature for 10 min prior to the reaction. Reactions were initiated by the addition of the enzyme/1–143 cocktail to the UDP-Gal-containing wells (90 μL of cocktail per well). Each concentration of UDP-Gal/1–143 was measured in duplicate. Initial rates were calculated as described previously. The data were fit by nonlinear regression analysis to a competitive inhibition model using SAS software (Cary, NC).

Purification of Human 4-Epimerase

The yeast strain JFY1023, which expresses the human 4-epimerase with a C-terminal His $_6$ tag, was prepared previously by Fridovich-Keil and coworkers and was a generous gift to us from that lab. Protocols for protein expression and purification are derived from those described previously [51, 52]. Cultures of JFY1023 yeast (4×1 liter) were grown at 30°C in minimal complete dextrose medium deficient in histidine (SD-His, Clontech 8602-1, 8606-1) to an OD(600 nm) = 0.6–0.8. Yeast cells were pelleted by centrifugation ($1000 \times g$, 5 min, 4°C) and either stored frozen at -80°C or used immediately. The following “purification buffer” was common to all subsequent steps: 20 mM HEPES (pH 7.5) (Sigma H0763), 200 mM NaCl, 4 mM β -NAD $^+$ (Sigma N1511), and $1 \times$ protease inhibitors. β -NAD $^+$ was included to stabilize the 4-epimerase. Protease inhibitors were stored as a $100 \times$ cocktail in DMSO and dispensed into the buffer immediately prior to use. The following compounds were included in the $100 \times$ cocktail: pepstatin A (Sigma P5318) at 100 $\mu\text{g}/\text{mL}$, aprotinin (Sigma A1153) at 210 $\mu\text{g}/\text{mL}$, leupeptin (Sigma L2884) at 50 $\mu\text{g}/\text{mL}$, antipain (Sigma A6191) at 260 $\mu\text{g}/\text{mL}$, phosphoramidon [N -(α -rhamnopyranosyloxyhydroxy-phosphinyl)-leu-trp, Sigma R7385] at 60 $\mu\text{g}/\text{mL}$, E64 [trans-epoxysuccinyl-L-leucylamido(4-guanidino)-butane, Sigma 3132] at 750 $\mu\text{g}/\text{mL}$, and chymostatin (Sigma C7268) at 10 $\mu\text{g}/\text{mL}$. A separate $100 \times$ solution of Pefabloc SC (Boehringer Mannheim 1429 868) at 24 mg/mL in DMSO was used as well. All steps of the purification protocol were performed either on ice or at 4°C , using prechilled buffers, to stabilize the 4-epimerase and minimize protease activity.

For preparation of the yeast extract, the yeast pellet was suspended in a minimum (5–10 mL) of purification buffer containing 25 mM imidazole at pH 7.5. The suspension was transferred to a 30

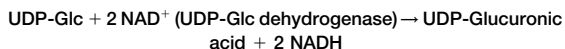
ml BioSpec Bead Beater bottle that had been half-filled with 0.5 mm glass beads (BioSpec 11079105). Additional purification buffer with 25 mM imidazole was used to rinse residual yeast into the bottle and to fill it to within 0.5 cm of its top. The Bead Beater was assembled, with crushed dry ice surrounding the bottle to keep its contents chilled. The Bead Beater was pulsed on for 2 min, then off for 30 s, for a total of six cycles; the 30 s intervals between pulses were designed to allow the bottle's contents to cool after they were warmed by beating. The yeast extract was separated from the glass beads by filtration through glass wool in a 60 ml plastic syringe; additional purification buffer with 25 mM imidazole was used to rinse the bottle and beads. The extract was centrifuged at 4°C (15000 × g, 15 min) to pellet cellular debris. If the resultant lysate was still opaque, centrifugation was repeated for 5 min.

Purification of the His₆-tagged 4-epimerase from the crude cell lysate was accomplished by loading the approximately 20 ml of fresh lysate directly onto a column of 5 ml Ni-NTA agarose (Qiagen 30210) that had been preequilibrated with purification buffer containing 25 mM imidazole. The column was loaded at 0.5 ml/min; ensuing washes and elutions were performed at 1.0 ml/min. The column was washed successively with purification buffer containing 25 mM imidazole (5 ml), 50 mM imidazole (20 ml), and 100 mM imidazole (10 ml). Fractions (5 ml) were collected from the column during loading and washing. The 4-epimerase was eluted with purification buffer containing 200 mM imidazole (20 ml); 2 ml fractions of the eluent were collected.

Column fractions were assayed for 4-epimerase activity using the same assay described above, with minor variations. Aliquots (10 µl) of column fractions were dispensed into a 96-well plate. A buffer cocktail containing the remaining assay reagents was prepared on ice, incubated at room temperature for 10 min prior to use, and then dispensed into the microplate at 90 µl/well. Final concentrations of reagents were as follows: 1.0 mM UDP-Gal; 16 mU UDP-Glc dehydrogenase; 1.25 mM β-NAD⁺; 125 mM potassium bicarbonate (pH 8.5). Absorbance at 340 nm was monitored for 5 min. While enzyme activity was observed in both the flow-through fractions and the 200 mM imidazole eluent, the former was nonspecific and was observed even in the absence of UDP-Gal or UDP-Glc dehydrogenase. The number of units of 4-epimerase present in active fractions was estimated by comparing rates to control samples containing known concentrations of the bacterial 4-epimerase. To these fractions, glycerol and β-NAD⁺ were added to final concentrations of 50% (vol/vol) and 4.0 mM, respectively. 4-Epimerase was stored immediately at -20°C, where it was stable for approximately 1 month. Glycerol solutions of 4-epimerase were used in subsequent assays at dilutions ranging from 10- to 50-fold, depending on the stock solution concentration. Overall, we found the human 4-epimerase to be much less stable than its bacterial counterpart; overnight dialysis to remove imidazole or freezing of aliquots in the absence of glycerol both ablated enzyme activity.

Spectrophotometric Assay for UDP-Glc Dehydrogenase Activity

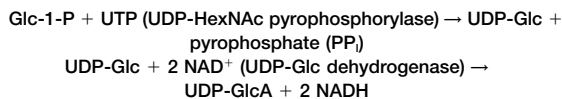
Activity of the UDP-Glc dehydrogenase was monitored as described by the equation below:



The production of NADH, and hence the activity of the dehydrogenase, was followed by measuring the absorbance at 340 nm. Assays were performed in an analogous manner to those for the 4-epimerase. Final concentrations of assay components were as follows: 20 µM UDP-Glc (equivalent to the K_m value); 12 mU UDP-Glc dehydrogenase; 1.25 mM NAD⁺; 125 mM potassium bicarbonate (pH 8.5). IC₅₀ measurements were performed in an analogous fashion to that described for the 4-epimerase; compound 1-143 was dispensed to the microplate, a solution containing the dehydrogenase was added, and the solution was incubated at room temperature until the absorbance achieved a stable baseline, and finally the reaction was initiated by the addition of UDP-Glc. Enzyme progress was monitored for 5 min, with readings every 3 s; the initial linear portion of the progress curve occurred within the first 45 s of the assay.

Spectrophotometric Assay for UDP-GlcNAc/GalNAc Pyrophosphorylase Activity

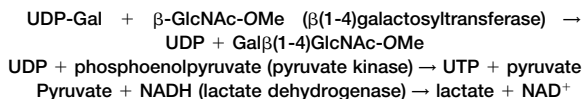
The UDP-HexNAc pyrophosphorylase, a porcine version of the enzyme expressed with a His₆ tag in *E. coli*, was a generous gift from Dr. Alan Elbein [53]. Activity of the UDP-HexNAc pyrophosphorylase was monitored as described by the equation below. Note that while the preferred substrates for this enzyme are the *N*-acetamido sugars—either GlcNAc-1-phosphate or GalNAc-1-phosphate—glucose-1-phosphate (Glc-1-P) is accepted as an alternative substrate, making possible the spectrophotometric assay described here.



Production of NADH served as a read-out of enzyme activity. Final concentrations of assay components were as follows: 200 µM UTP (equivalent to the K_m value); 20 mM Glc-1-P (equivalent to three times the K_m value); 267 mU UDP-Glc dehydrogenase; 5.0 mM NAD⁺; 80 mM Tris-HCl (pH 7.5); 5.0 mM MgCl₂; and 0.05–0.1 mU UDP-HexNAc pyrophosphorylase. IC₅₀ measurements were performed in a similar fashion to those described previously. Initial rates and percent inhibition of enzyme activity were calculated as described for the 4-epimerase.

Spectrophotometric Assay for β(1-4) Galactosyltransferase Activity

Activity of the β(1-4)galactosyltransferase was monitored using a coupled enzyme assay as summarized below [53]:



The disappearance of NADH, and thus galactosyltransferase activity, was monitored at 340 nm. Final concentrations of assay components were as follows: MgCl₂, 10 mM; MnCl₂, 5 mM; KCl, 50 mM; phosphoenolpyruvate (monocyclohexylammonium salt, Sigma P3637), 1.5 mM; potassium bicarbonate (pH 8.5), 50 mM; NADH (Sigma 340-105), 0.2 mM; β-GlcNAc-OMe, 4 mM; pyruvate kinase (Sigma, P9136), 150 mU; lactate dehydrogenase (Calbiochem 427217), 150 mU; (β1-4)galactosyltransferase (Calbiochem 345649), 0.1 mU; UDP-Gal, 100 µM, the K_m concentration. Assay components were assembled on ice in the order listed, with the requisite amount of water added first. Enzyme solutions and NADH were prepared fresh just prior to the assay. It was important that the phosphoenolpyruvate be sufficiently buffered, as an acidic solution would cause decomposition of the NADH. Normally, the phosphoenolpyruvate was prepared as a 10× stock solution in 10× potassium bicarbonate. The pH of the reaction mixture was measured prior to NADH addition. IC₅₀ measurements were performed in an analogous manner to that described for the 4-epimerase.

Acknowledgments

We thank Joshua I. Armstrong for insights into library design and synthesis and for assistance with analysis of kinetic data. We thank Michelle Dudley for assistance with molecular modeling and Monica Palcic for helpful advice on the β(1-4)galactosyltransferase assay. We thank Jonathan Ellman and his coworkers for numerous helpful discussions. The authors are grateful for generous funding from Merck and the Research Corporation. This research was supported by a grant to C.R.B. from the National Science Foundation (CHE-9734430).

References

- Ellies, L.G., Tsuboi, S., Petryniak, B., Lowe, J.B., Fukuda, M., and Marth, J.D. (1998). Core 2 oligosaccharide biosynthesis distinguishes between selectin ligands essential for leukocyte homing and inflammation. *Immunity* 9, 881–890.

2. Dasgupta, A., Takahashi, K., Cutler, M., and Tanabe, K.K. (1996). O-Linked glycosylation modifies CD44 adhesion to hyaluronate in colon carcinoma cells. *Biochem. Biophys. Res. Commun.* 227, 110–117.
3. Takasaki, S., Mori, E., and Mori, T. (1999). Structures of sugar chains included in mammalian *zona pellucida* glycoproteins and their potential roles in sperm-egg interaction. *Biochim. Biophys. Acta* 1473, 206–215.
4. Dennis, J.W., Granovsky, M., and Warren, C.E. (1999). Protein glycosylation in development and disease. *Bioessays* 21, 412–421.
5. van Zuylen, C.W., Kamerling, J.P., and Vliegenthart, J.F. (1997). Glycosylation beyond the Asn78-linked GlcNAc residue has a significant enhancing effect on the stability of the α -subunit of human chorionic gonadotropin. *Biochem. Biophys. Res. Commun.* 232, 117–120.
6. Barbier, O., Girard, C., Breton, R., Bélanger, A., and Hum, D.W. (2000). N-Glycosylation and residue 96 are involved in the functional properties of UDP-glucuronosyltransferase enzymes. *Biochemistry* 39, 11540–11552.
7. Howard, S.C., Wittwer, A.J., and Welpy, J.K. (1991). Oligosaccharides at each glycosylation site make structure-dependent contributions to biological properties of human tissue plasminogen activator. *Glycobiology* 1, 411–418.
8. Elhammer, A.P., Kézdy, F.J., and Kurosaka, A. (1999). The acceptor specificity of UDP-GalNAc:polypeptide N-acetylgalactosaminyltransferases. *Glycoconj. J.* 16, 171–180.
9. Marth, J.D. (1996). Complexity in O-linked oligosaccharide biosynthesis engendered by multiple polypeptide N-acetylgalactosaminyltransferases. *Glycobiology* 6, 701–705.
10. Sadeghi, H., and Birnbaumer, M. (1999). O-Glycosylation of the V2 vasopressin receptor. *Glycobiology* 9, 731–737.
11. Kuan, S.F., Byrd, J.C., Basbaum, C., and Kim, Y.S. (1989). Inhibition of mucin glycosylation by aryl-N-acetyl- α -galactosaminides in human colon cancer cells. *J. Biol. Chem.* 264, 19271–19277.
12. Elbein, A.D. (1987). Inhibitors of the biosynthesis and processing of N-linked oligosaccharide chains. *Annu. Rev. Biochem.* 56, 497–534.
13. Eason, P.D., and Imperiali, B. (1999). A potent oligosaccharyl transferase inhibitor that crosses the intracellular endoplasmic reticulum membrane. *Biochemistry* 38, 5430–5437.
14. White, K.E., Lorenz, B., Evans, W.E., Meitinger, T., Strom, T.M., and Econs, M.J. (2000). Molecular cloning of a novel human UDP-GalNAc:polypeptide N-acetylgalactosaminyltransferase, GalNAc-T8, and analysis as a candidate autosomal dominant hypophosphatemic rickets (ADHR) gene. *Gene* 246, 347–356.
15. Smith, P.L., Kaetzel, D., Nilson, J., and Baenziger, J.U. (1990). The sialylated oligosaccharides of recombinant bovine lutropin modulate hormone bioactivity. *J. Biol. Chem.* 265, 874–881.
16. Smith, P.L., Skelton, T.P., Fiete, D., Dharmesh, S.M., Beranek, M.C., MacPhail, L., Broze, G.J., Jr., and Baenziger, J.U. (1992). The asparagine-linked oligosaccharides on tissue factor pathway inhibitor terminate with SO₄-4GalNAc β 1–4 GlcNAc β 1–2 Man α . *J. Biol. Chem.* 267, 19140–19146.
17. Smith, P.L., Bousfield, G.R., Kumar, S., Fiete, D., and Baenziger, J.U. (1993). Equine lutropin and chorionic gonadotropin bear oligosaccharides terminating with SO₄-4-GalNAc and Sia α 2–3 Gal, respectively. *J. Biol. Chem.* 268, 795–802.
18. Krieger, M., Reddy, P., Kozarsky, K., Kingsley, D., Hobbie, L., and Penman, M. (1989). Analysis of the synthesis, intracellular sorting, and function of glycoproteins using a mammalian cell mutant with reversible glycosylation defects. *Methods Cell Biol.* 32, 57–84.
19. Kingsley, D.M., Kozarsky, K.F., Hobbie, L., and Krieger, M. (1986). Reversible defects in O-linked glycosylation and LDL receptor expression in a UDP-Gal/UDP-GalNAc 4-epimerase deficient mutant. *Cell* 44, 749–759.
20. Piller, F., Hanlon, M.H., and Hill, R.L. (1983). Co-purification and characterization of UDP-glucose 4-epimerase and UDP-N-acetylglucosamine 4-epimerase from porcine submaxillary glands. *J. Biol. Chem.* 258, 10774–10778.
21. Rudd, P.M., and Dwek, R.A. (1997). Glycosylation: heterogeneity and the 3D structure of proteins. *Crit. Rev. Biochem. Mol. Biol.* 32, 1–100.
22. Wang, R., Steensma, D.H., Takaoka, Y., Yun, J.W., Kajimoto, T., and Wong, C.H. (1997). A search for pyrophosphate mimics for the development of substrates and inhibitors of glycosyltransferases. *Bioorg. Med. Chem.* 5, 661–672.
23. Hashimoto, H., Endo, T., and Kajihara, Y. (1997). Synthesis of the first tricomponent bisubstrate analogue that exhibits potent inhibition against GlcNAc: β 1,4-galactosyltransferase. *J. Org. Chem.* 62, 1914–1915.
24. Yuasa, H., Palcic, M.M., and Hindsgaul, O. (1995). Synthesis of the carbocyclic analog of uridine 5'-(α -D-galactopyranosyl diphosphate) (UDP-Gal) as an inhibitor of β (1–4)-galactosyltransferase. *Can. J. Chem.* 73, 2190–2195.
25. Palcic, M.M., Heerze, L.D., Srivastava, O.P., and Hindsgaul, O. (1989). A bisubstrate analog inhibitor for α (1–2)-fucosyltransferase. *J. Biol. Chem.* 264, 17174–17181.
26. Muller, B., Schaub, C., and Schmidt, R.R. (1998). Efficient sialyltransferase inhibitors based on transition-state analogues of the sialyl donor. *Angew. Chem. Int. Ed. Engl.* 37, 2893–2897.
27. Canne, L.E., Ferredamare, A.R., Burley, S.K., and Kent, S.B.H. (1995). Total chemical synthesis of a unique transcription factor-related protein - cMyc-Max. *J. Am. Chem. Soc.* 117, 2998–3007.
28. Rose, K. (1994). Facile synthesis of homogeneous artificial proteins. *J. Am. Chem. Soc.* 116, 30–33.
29. Mahal, L.K., Yarema, K.J., and Bertozzi, C.R. (1997). Engineering chemical reactivity on cell surfaces through oligosaccharide biosynthesis. *Science* 276, 1125–1128.
30. Lemieux, G.A., Yarema, K.J., Jacobs, C.L., and Bertozzi, C.R. (1999). Exploiting differences in sialoside expression for selective targeting of MRI contrast reagents. *J. Am. Chem. Soc.* 121, 4278–4279.
31. Maly, D.J., Choong, I.C., and Ellman, J.A. (2000). Combinatorial target-guided ligand assembly: identification of potent subtype-selective c-Src inhibitors. *Proc. Natl. Acad. Sci. USA* 97, 2419–2424.
32. Thoden, J.B., and Holden, H.M. (1998). Dramatic differences in the binding of UDP-galactose and UDP-glucose to UDP-galactose 4-epimerase from *Escherichia coli*. *Biochemistry* 37, 11469–11477.
33. Camarasa, M.J., Fernández-Resa, P., García-López, M.T., de las Heras F.G., Méndez-Castrillón, P.P., Alarcón, B., and Carasco, L. (1985). Uridine 5'-diphosphate glucose analogues. Inhibitors of protein glycosylation that show antiviral activity. *J. Med. Chem.* 28, 40–46.
34. Radominska, A., Paul, P., Treat, S., Towbin, H., Pratt, C., Little, J., Magdalou, J., Lester, R., and Drake, R. (1994). Photoaffinity labeling for evaluation of uridyl analogs as specific inhibitors of rat liver microsomal UDP-glucuronosyltransferases. *Biochim. Biophys. Acta* 1205, 336–345.
35. Traxler, P.M., Wacker, O., Bach, H.L., Geissler, J.F., Kump, W., Meyer, T., Regenass, U., Roesel, J.L., and Lydon, N. (1991). Sulfonylbenzoyl-nitrostyrenes: potential bisubstrate type inhibitors of the EGF-receptor tyrosine protein kinase. *J. Med. Chem.* 34, 2328–2337.
36. Shuker, S.B., Hajduk, P.J., Meadows, R.P., and Fesik, S.W. (1996). Discovering high-affinity ligands for proteins: SAR by NMR. *Science* 274, 1531–1534.
37. Rodríguez, E.C., Winans, K.A., King, D.S., and Bertozzi, C.R. (1997). A strategy for the chemoselective synthesis of O-linked glycopeptides with native sugar-peptide linkages. *J. Am. Chem. Soc.* 119, 9905–9906.
38. Karabatsos, G.J., and Hsi, N. (1967). Structural studies by nuclear magnetic resonance—XI. Conformations and configurations of oxime O-methyl ethers. *Tetrahedron* 23, 1079–1095.
39. Uno, T., Gong, B., and Schultz, P.G. (1994). Stereoselective antibody-catalyzed oxime formation. *J. Am. Chem. Soc.* 116, 1145–1146.
40. (1993). RNA metabolism. In *Principles of Biochemistry*, A.L. Lehninger, D.L. Nelson, and M.M. Cox, eds. (New York: Worth Publishers), pp. 856–889.
41. Ernst, B., and Oehlein, R. (1999). Substrate and donor specificity of glycosyltransferases. *Glycoconj. J.* 16, 161–170.
42. Butler, T., and Elling, L. (1999). Enzymatic synthesis of nucleotide sugars. *Glycoconj. J.* 16, 147–159.
43. Platt, F.M., Neises, G.R., Reinkensmeier, G., Townsend, M.J.,

- Perry, V.H., Proia, R.L., Winchester, B., Dwek, R.A., and Butters, T.D. (1997). Prevention of lysosomal storage in Tay-Sachs mice treated with *N*-butyldeoxynojirimycin. *Science* 276, 428–431.
44. Poolman, B., Royer, T.J., Mainzer, S.E., and Schmidt, B.F. (1990). Carbohydrate utilization in *streptococcus thermophilus*: characterization of the genes for aldose 1-epimerase (mutorotase) and UDP-glucose 4-epimerase. *J. Bacteriol.* 172, 4037–4047.
45. Cunha, B.A. (1993). Aztreonam. *Urology* 41, 249–258.
46. Wilde, M.I., Plosker, G.L., and Benfield, P. (1993). Fluvoxamine. An updated review of its pharmacology, and therapeutic use in depressive illness. *Drugs* 46, 895–924.
47. Thoden, J.B., Wohlers, T.M., Fridovich-Keil, J.L., and Holden, H.M. (2000). Crystallographic evidence for Tyr 157 functioning as the active site base in human UDP-galactose 4-epimerase. *Biochemistry* 39, 5691–5701.
48. Sarkar, A.K., Fritz, T.A., Taylor, W.H., and Esko, J.D. (1995). Disaccharide uptake and priming in animal cells - inhibition of sialyl Lewis X by acetylated Gal- β -1-4GlcNAc- β -O-naphthalenemethanol. *Proc. Natl. Acad. Sci. USA* 92, 3323–3327.
49. Hofman-Bang, N. (1957). Preparation of lithium azide. *Acta Chem. Scand.* 11, 581–582.
50. Budesinsky, M., and Exner, O. (1989). Correlation of Carbon-13 substituent-induced chemical shifts – *meta*-substituted and *para*-substituted methyl benzoates. *Magn. Reson. Chem.* 27, 585–591.
51. Fridovich-Keil, J.L., and Jinks-Robertson, S. (1993). A yeast expression system for human galactose-1-phosphate uridylyltransferase. *Proc. Natl. Acad. Sci. USA* 90, 398–402.
52. Quimby, B.B., Alano, A., Almashanu, S., DeSandro, A.M., Cowan, T.M., and Fridovich-Keil, J.L. (1997). Characterization of two mutations associated with epimerase-deficiency galactosemia, by use of a yeast expression system for human UDP-galactose-4-epimerase. *Am. J. Hum. Genet.* 61, 590–598.
53. Wang-Gillam, A., Pastuszak, I., and Elbein, A.D. (1998). A 17-amino acid insert changes UDP-*N*-acetylhexosamine pyrophosphorylase specificity from UDP-GalNAc to UDP-GlcNAc. *J. Biol. Chem.* 273, 27055–27057.
54. Gosselin, S., Alhussaini, M., Streiff, M.B., Takabayashi, K., and Palcic, M.M. (1994). A continuous spectrophotometric assay for glycosyltransferases. *Anal. Biochem.* 220, 92–97.